The International Journal of Advanced Manufacturing Technology
https://doi.org/10.1007/s00170-022-08840-x

CRITICAL REVIEW

Laser polishing: a review of a constantly growing technology in the surface finishing of components made by additive manufacturing

Gisario Annamaria[1] · **Barletta Massimiliano**[2] · **Veniali Francesco**[1]

Received: 20 November 2021 / Accepted: 27 January 2022

Abstract
Additive manufacturing is a vanguard production technology that has contributed greatly to speed up replacing on the market of complex-shaped components. A delicate and unavoidable phase of additive technology is that relating to the post-processing of the components, especially the finishing process. Post-processing needs to be automated and made scalable so that the technology can actually be adopted also for mass production. In this respect, an emerging post-processing technology suitable for surface finishing, not in contact and easily automatable, is the one that involves the use of laser sources, known by the name of laser polishing. Laser polishing is spreading, in fact, more and more strongly, in the field of manufacturing as a valid alternative to conventional technologies for the surface finishing of metallic components obtained by additive processes. Laser polishing is widely considered very suitable to improving the surface finish of metal components. When compared with the conventional finishing technologies, laser polishing has many benefits in terms of costs and process times especially if automated, through the use of CNC systems and scanning heads. In this manuscript, the knowledge of this technology is deepened through a review of the relevant literature that highlights the aspects of the interaction of the laser beam with the metal alloys most frequently used in 3D printing, without neglecting the importance of the thermo-mechanical properties that derive from it. The analysis conducted on the technology of laser polishing aims therefore at evaluating the potential applications in industrial engineering, mainly with regard to the surfaces quality achievable as a result of the polishing of metal components fabricated by additive manufacturing.

Keywords Laser polishing · Additive manufacturing · 3D printing · Surface finishing · Surface roughness

1 Introduction

The term additive manufacturing (AM) refers, as is known, to a set of fabrication technology whose common characteristic is to manufacture a particular component by adding material, layer by layer, only where it is necessary, starting from digital data and a 3D CAD virtual model [1–8]. By comparing AM with traditional fabrication technologies, it can be seen that the design phase of the production process is considerably simplified and shortened. A traditional process would require a careful analysis of the geometry of the component to decide the order in which the machining macrocycles must be carried out, the choice of tools, the choice of the individual technologies to use, and the manufacture of the necessary equipment (for example, the molds and the inserts) [3].

In contrast, in any AM process, as shown in Fig. 1, it is only necessary to consider a predetermined number of common steps to obtain the final part [3]. Step 1 - 3D model: first, a 3D model of the object is created using CAD software or a 3D object scanner,step 2 - STL file: CAD model is converted to a STL file to tessellate the 3D shape and slice it into digital layers; step 3 - STL file transfer: STL file is then transferred to the printer using custom machine software; step 4 - machine set up: consumables are then loaded and the printer is set up with printing parameters; step 5 - building: printer builds the model by depositing

✉ Barletta Massimiliano
massimiliano.barletta@uniroma3.it

[1] Dipartimento di Ingegneria Meccanica e Aerospaziale, Sapienza Università di Roma, Via Eudossiana 18, 00184 Rome, Italy

[2] Dipartimento di Ingegneria Industriale, Elettronica e Meccanica, Università degli Studi Roma Tre, Via della Vasca Navale 79, 00146 Rome, Italy

Published online: 21 February 2022

Fig. 1 Generic steps in additive manufacturing

material layer by layer; step 6 - part removal: part is then removed from the build platform and its support structure; step 7 - post-processing: post-processing, such as cleaning, polishing, and painting, might be, eventually, required. The laser polishing technology therefore intervenes in the final post-processing step.

In recent years, there has been a notable development of additive technologies as they allow the manufacture of components with very intricate geometries and also of large dimensions. The advances achieved in additive technology make it possible to produce objects with speeds that are not often related to their complexity, and it is possible to choose from multiple combinations of materials, colors, and finishes.

Since the first patent granted in 1986 [9] and the first 3D printing machine (based on stereolithography) built in the late 1980s by 3D Systems, the AM industry market has grown significantly in the first decade (~ $1 billion US - 1997). At the same time, the AM industry has moved from rapid prototyping to functional prototyping. Today, additive technology is used in all sectors of industry, from aerospace to the biomedical sector and from toys to food sector, and represents a multi-billion dollar industry [10].

The ASTM (American Society of Testing and Materials) has grouped all additive manufacturing processes into 7 different categories [11]. The most relevant categories in which there are technologies that process metallic materials are category 5 called "powder bed fusion," that is, selective laser sintering (SLS), selective laser melting (SLM), and electron beam melting (EBM) technologies and category 7 called "direct energy deposition," that is, laser engineered net shaping (LENS) technology, also known as direct metal deposition (DMD), direct laser deposition (DLD), and additive laser manufacturing (ALM). For the fabrication of metal components, of medium and small dimensions, the most used technologies to date are SLM and EBM [12–19]. For both technologies, manufacturing has, as its starting point, metallic powders that are characterized on the basis of shape (circularity) and particle size distribution by using image analysis and laser diffraction [20]. With the metal powders, a thin layer is developed on the building platform and, through an energy source (laser or electron beam), the material is selectively melted in the affected areas to form one of the layers of which the final object will be composed of. Once the layer has been melted and resolidified, a new bed of powder is deposited and, by iterating the process, the final product will be obtained. The quality of the surfaces obtained is influenced by many factors. One of the most important process parameters is the orientation of the component on the building platform and has a great impact on the achievable roughness [21]. In fact, it has been seen that, for SLM and EBM technologies, the surfaces facing

downwards and the vertical surfaces are of lower quality, while the surfaces facing upwards have lower roughness values [22, 23]. Another fundamental factor for additive manufacturing is the generation of the building supports [24]. In particular, for SLM technologies, the support structures have different functions. They are necessary for the correct cooling of the components as they offer a way to the heat that must be dissipated,they allow to guarantee the position of the component on the building platform in a stable way, avoid distortions due to the coater that deposits the subsequent layers of powder, avoid annoying distortions that occur due to internal thermal stresses, and support the cantilevered structures. For protruding structures, supports are necessary as metal powder alone could lead to the formation of percolations of the liquid metal and also to overheating of the adjacent area, compromising the quality of the surface [22]. In Fig. 2, a titanium cabin bracket built for the Airbus A350 XWB by the SLM process is reported. For this component, Childerhouse and Jackson [24] demonstrated how the design and positioning of support structures, as well as the orientation of the part on the building platform, influence the thermal strains induced in the component.

However, once the object was manufactured, the support structures must be removed and the removal, whether manual for very small structures, or using tools, can compromise the surface quality of the component.

In powder bed fusion (PBF) processes, the melting of metal powders is involved. Therefore, during laser scanning, pyroclastic flows and vaporizations of small portions of material are continuously generated, which then re-solidify and consolidate on already manufactured parts, thus contributing to the generation of defects. In addition, incomplete melting processes may occur during the process due to incorrect powder bed development. Accordingly, protrusions can be formed due to the motion of the molten material, thus generating defects that are referred to as "balling" [25]. Adopting too high scanning powers and speeds, the molten material tends to assume a spherical configuration, causing the formation of a non-homogeneous surface. Many scientific works in the literature show the influence of all process parameters on the elimination of defects that compromise the quality of the surface of the end-product [26–33]. However, although it is possible to intervene in the optimization phase of the process parameter, since AM is a technology that allows the manufacture of layer-by-layer components, the surface of the aforementioned components will always result from a stepped morphology, characterized by the superimposition of the different manufacturing layers. This effect can certainly be reduced by decreasing the height of the single layer, but it cannot be completely eliminated. Furthermore, in SLM and EBM, the powders are selectively melted and the energy is focused on a small

Fig. 2 Airbus A350 XWB cabin bracket built by GE Additive's LaserCUSING R SLM additive manufacturing process [24]

spot. This also leads to a partial sintering of the powders adjacent to the surface [34]. These powder grains cause a high surface roughness of the end-product. Post-processing treatments, such as grinding, polishing, and sometimes even shot peening, can be used to improve the surface finish of the end-products. With the available thickness of the layers of the equipments that are nowadays available on the market, the surface roughness obtainable with an SLM process is, on average, included in a range that goes from about 4 to 30–40 µm, while for an EBM process, the range is greater, i.e., 25 to 130 µm [35, 36]. Obviously, these are indicative values since they strongly depend on the main process parameters chosen in the two technologies involved. For example, Fig. 3 shows images of scaffolds manufactured in Ti6Al4V by SLM and EBM by Weißmann et al. [37] according to two distinct orientations: 0° and 45°. The SLM parts show greater precision than the EBM parts, and with regard to surface roughness, it is shown that the values of the R_a and R_z indices are significantly lower along both the directions and agree with those reported in the literature [37]. By progressively increasing the inclination angle from 0°, a greater surface roughness, in SLM parts, is found because of the "stair–step" effect [38].

Obtaining a good quality of the surface finish therefore remains a crucial problem in manufacturing using additive technologies that process metallic materials and requires, for many applications, lengthy post-processing operations that are made more difficult in case of high geometric complexity of the component.

2 The growing use of laser technology in polishing operations

During the manufacture of a mechanical component, it is of paramount importance to comply with the requirements in terms of dimensional or geometric tolerances and surface morphology. In particular, from a technological point of view, it is necessary to understand how to create surfaces according to the task that the surface itself will have to perform [39]. A mechanical component, during its useful life, will be part of couplings that can be static or dynamic. For static couplings, tolerance and surface roughness constraints must be respected. For dynamic mates, perfect sliding surfaces must be satisfied. Consequently, a suitable morphological profile of the surface must be guaranteed during manufacturing, suitable for lubrication and which allows to prevent wear and loss of tolerance. Usually, for mechanical couplings, functional surfaces have quite stringent roughness requirements since a profile that has many ridges could favor fatigue failure, as it has numerous stress intensification points [40–43]. The roughness parameter assumes an important meaning even if the corrosion phenomenon is considered. In fact, a smoother roughness profile can reduce the tendency of the product to corrode [44]. The evaluation of surface roughness is important not only for many problems, including the regulation of friction and wear phenomena, but also for electrical conductivity problems [45]. Sometimes the surface finish requirement can also be an aesthetic one, even if a functional surface is not required. It is very complicated to have a complete description of the real surface with a limited number of parameters. In general, those commonly used can be divided into three broad categories: parameters of amplitude, spacing, and hybrid parameters [39, 46]. Each production process has limits in terms of obtainable roughness, and therefore, the choice will depend on the technical specifications to be met. For traditional processes, such as turning or milling, there are different models that can allow predicting roughness [47–54]. More stringent requirements on roughness parameters, surface finishing, or superfinishing technologies will be used in most critical zones of the components. For AM processes, many researchers have proposed predictive roughness models [38, 55, 56] that take into account both the "stair step effect," the defects deriving from the phenomenon of balling (i.e., a phenomenon in which spherical droplets are formed due to the

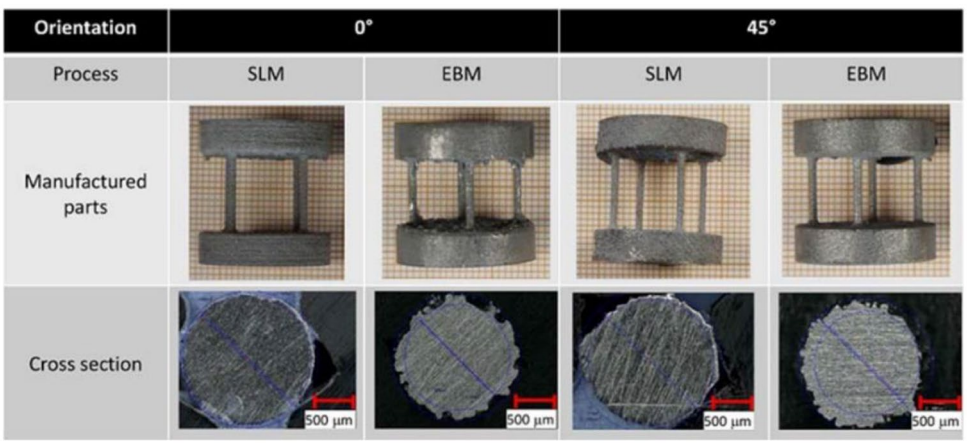

Fig. 3 Examples of scaffolds produced via SLM and EBM [37]

insufficient wettability of the molten metal with the underlying layer) as well as to the presence of satellites (i.e., very small particles attached to the surface of larger ones). Since AM technology has intrinsic limits, it is necessary to deepen in detail the so-called post-processing technologies of the components produced by AM. The amplitude of the building volume (that is, of the work area) of AM equipment currently on the market is not very high, so the components are limited in size. Thanks to the specific features of AM technologies, these components have very complex geometries. These can be obtained by topological optimization [57, 58] or because they have internal latex type structures [59–62], which confer unique properties to the components but, at the same time, limited accessibility to their surface. It would be very complicated to use conventional finishing technologies on latex structures or, in any case, on structures characterized by very complex geometries. The conventional finishing technique widely recognized for such purposes is the barrel finishing that uses abrasive media and constitutes a mass finishing process [63]. However, the processing times are to be considered rather long and sometimes in contrast with the current production needs, especially when the number of pieces to be processed is limited. In this regard, one of the most suitable technologies to date for finishing small components with complex geometry is laser polishing. This technology constitutes a new approach to polishing metal surfaces and has advantages over, for example, sandblasting, tumbling, grinding, and polishing by electrochemical media since there is no formation of chips or, more generally, of by-products. In addition, processing does not involve tools which would require a continuous replacement, which could also cause the formation of tracks or scratches on the material. The processing takes place without effective contact between the source and the product and can count on a good level of automation, a feature that makes it even more attractive for industrial applications.

The polishing of metals by means of laser is based on melting and resolidification (remelting) of a thin layer of material on the surface to be polished. The interaction of the laser beam with the surface of the material allows the creation of a molten pool of the material itself which, guided by the surface tension, is redistributed in the adjacent area, contributing to an improvement in the surface finish.

Laser polishing processes include the following: (i) pulsed laser sources; (ii) continuous laser sources; (iii) combinations of pulsed and continuous laser sources; (iv) selective laser polishing techniques [64]. The pulsed sources are generally used in the micro-polishing of surfaces [65]. Pulsed sources are based on discrete low power pulses that irradiate the metal surface once, generating a pool of molten metal affecting domains of the order of 10–100 nm [66]. The resolidification of the material takes place before the next irradiation. It is possible to adjust the duration and frequency of the pulses, allowing a fine control of the polishing process [67, 68]. Continuous sources, on the other hand, are used for polishing macro-surfaces [69]. The polishing process is continuous, that is, obtained by irradiating the surface with a continuous laser beam. The pool of molten metal that can be obtained depends on the diameter of the beam, the average power (in general, much higher than pulsed sources), and the scanning speed of the beam [70]. This type of process is used on surfaces characterized by R_a 2–16 microns, with the melting involving 20–200 microns of surface exposed to the beam, with the aim of obtaining an average roughness R_a after the laser polishing treatment of about 0.1 microns. The powers typically involved vary between 70 and 300 W, with scanning speeds that can exceed 100 mm/s [64]. The combination of pulsed and continuous sources is done by installing a Q-Switch ([71, 72]. In general, this processing involves a first step in continuous source mode to homogenize the metal surface. This is followed by a sequence of interventions in pulsed mode to improve the finishing of details, making it possible to obtain finishes that cannot be achieved through the use of a single type of laser source [73]. Finally, the laser can be used to perform selective polishing of components unlike other finishing/polishing techniques, as only the areas to be improved can be exposed to the laser beam, without the need for masking ([71, 72]. This differentiates laser polishing techniques from mechanical techniques, as the latter cannot act selectively unless a preventive masking of the areas that must not be modified is carried out.

One of the first research on the use of technology in metal polishing was addressed by Ramos et al. [74], being encouraged by the interesting results obtained by Temple et al. [75] on fused silica surfaces and Wang et al. [76] on semiconductors. The laser had proved an excellent tool for surface modification of silica rods, the latter being able to be polished from 2.0 to 0.05 mm (i.e., peak-to-valley height) using a CO_2 laser source, operating in continuous mode, with a power of 25 W [76]. In order to modify the surface roughness of parts obtained by indirect SLS and manufactured with 420 stainless steel powder infiltrated with bronze, Ramos et al. [74] used two laser sources: CO_2 and Nd:YAG equipped with rotating mirrors driven by a high-speed galvanometric motor, with which it was possible to set the scanning speeds of up to 45 m/min. The authors identified two different mechanisms (Fig. 4): the surface shallow melting (SSM) and the surface over melt (SOM). In the first, the melting of the crests allows to reach lower roughness values, by means of the pouring of the molten material into the valleys. The capillary pressure minimizes the curvature between the bumps, allowing the molten material to flow into the lower pressure zone, helped by the reduction of its viscosity. In the second, an excessive surface melting, beyond to the removal of the original roughness, leads to the formation of capillary waves or surface ripples which develop in the

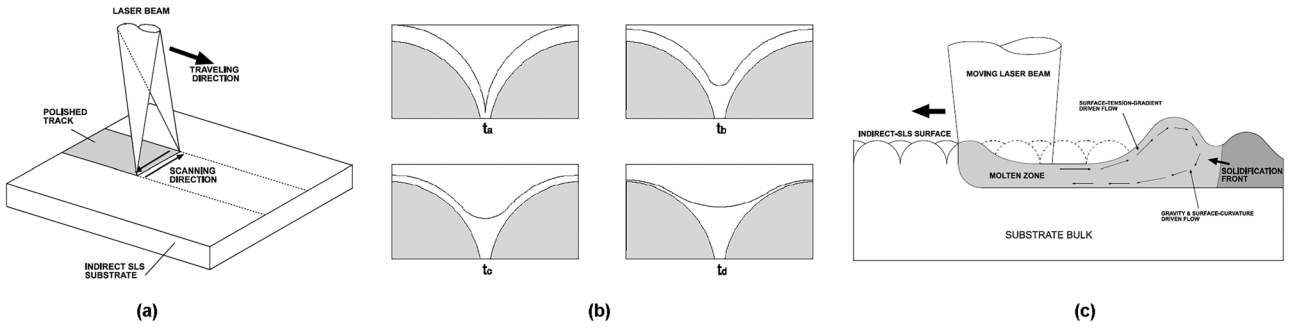

Fig. 4 Schematic diagram of the irradiation process in laser polishing. (**a**) Schematic of a surface structure formation during, (**b**) surface shallow melting (SSM) mechanism, and (**c**) surface over melt (SOM) mechanism [77]

direction perpendicular to the laser displacement due to a surface tension gradient behind the advancing laser beam. Their rapid resolidification phase causes an increase in the roughness [77].

Other researchers investigated laser polishing proposing preliminary predictive models to set the main process parameters [78] and testing the effect of the laser sources, operating both in pulsed [65, 69] and continuous mode [79–81], on roughness profiles generated by different machining processes, such as milling [82], electro-erosion [81], and sintering [83, 84], so as to verify the polishing effectiveness of the laser beam in various manufacturing contexts.

Laser polishing is to be considered specific for the creation of ultra-fine surfaces with variable characteristics, from simple to very complex. It turns out to be a combination of different thermophysical phenomena superimposed on each other. The main obstacle in the laser polishing process is represented by the difficulty in correctly selecting the various input finishing parameters in order to obtain the best output responses, such as the nanosurface roughness. More recently, Mohajerani et al. [85] and Purushothaman and Ravi Sankar [86] have attempted to model the laser polishing mechanism with greater accuracy, based on three laser polishing models: theoretical model, statistical model, and simulation of molecular dynamics to determine the relationship between the various processing parameters and the roughness of the final surface. Finite element modeling was also addressed [87] to study how heat transfer, fluid flow, and material vaporization are related to influence the evolution of surface topography in laser polishing. Among the surface forces, the capillary force of the molten pool is considered the main driving force for improving the surface finish. However, many uncertainties still exist in these studies that require additional investigation.

Other researchers have investigated more thoroughly [88], [68, 71–73] laser polishing, providing some valid theories on how to operate effectively and set the process parameters to obtain surfaces with a high quality. This allowed to pose the basis for the implementation of a CNC machine for laser polishing using the funding of 2 European projects: the EU poliMATIC and the BMBF ALPINE project. This sets the milestone for a new frontier in the process of polishing or surface smoothing of complex shape metal components, driving the direction of subsequent studies.

Most of the scientific works available today in the literature refer not only to laser polishing processes but also to those of metal surface structuring. In general, laser processes differ fundamentally from traditional processes (turning, milling, photochemical etching, etc.) in that the modification of the surface is performed by ablation of the material and/or redistribution of the material. Figure 5a, d show schematic representations of the physical principle underlying these processes.

Polishing processes can be classified as follows: macro-polishing and micro-polishing [71, 72], while surface structuring processes can be classified in wave shape [90] and structuring by recoil pressure [89].

2.1 Macro-laser polishing

In the macro-polishing process, a laser source is used which delivers the power continuously over time and the laser beam is moved across the surface of the component with a scanning speed v_s as shown in Figure 5a. Consequently, a pool of molten material will form which, by re-solidifying, will be distributed more homogeneously, reducing the irregularity of the initial surface. Two different areas can be distinguished in the processed surface. The first is the "remelted layer" that is the portion of material that is actually melted due to the interaction with the beam. In processes where a continuous source is used, this thickness can vary from 20 to 200 µm. The second zone is the thermally altered zone underlying the molten layer, and it is of fundamental importance since, depending on the material that is subjected to laser polishing, it can undergo phase transformations. This aspect will be, however, analyzed later.

The main process parameters in the case of macro-polishing are:

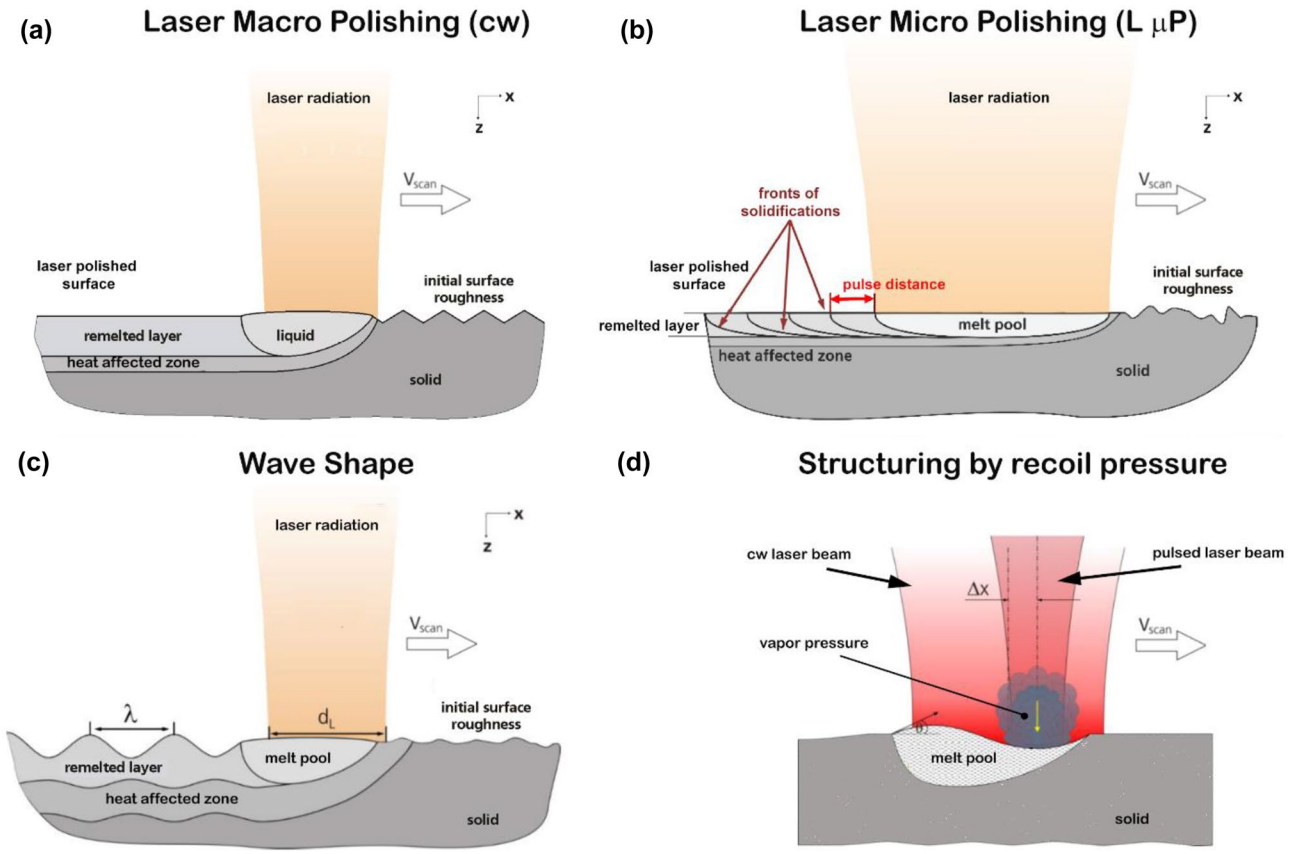

Fig. 5 Laser polishing and laser surface structuring processes: (**a**) laser macro-polishing (**b**) laser micro-polishing (**c**) laser wave shape (**d**) laser structuring by recoil pressure (reproduced from [71, 72, 89, 90])

P (W)	power carried by the LASER beam
v_s (mm/s)	scan rate
b (mm)	width of the track (laser scanning pattern)
h_s (mm)	distance between the centers of two adjacent tracks
p_{gas} (bar)	shield gas pressure

2.2 Micro-laser polishing

In the micro-polishing process, on the other hand, pulsed power sources are used. The single laser pulse hits the surface of the component creating a small pool of molten material (Fig. 5b). The laser pulses are short, lasting microseconds or nanoseconds. By combining the various parameters such as pulse frequency and scanning speed, it is possible to obtain the melting of a small portion of material at a time. In fact, when the pulse n reaches the surface of the component, the pool of molten material due to the pulse $n-1$ is already in a solid state. The molten zone has depths that do not exceed 5 μm, and, together with the melting, it is also possible to obtain a partial vaporization of the peaks constituting the initial surface. Also, in this case, there will be the generation of a thermally altered zone that must be controlled for the same reasons highlighted above.

P (W)	power carried by the LASER beam
v_s (mm/s)	scan rate
b (mm)	width of the track (laser scanning pattern)
h_s (mm)	distance between the centers of two adjacent tracks
p_{gas} (bar)	shield gas pressure
t_{on} (ns)	laser irradiation time
f (Hz)	pulse frequency

2.3 Wave shape

The Wave Shape structuring technology (see Fig. 5c) was first introduced by Temmler et al. [90] and is based on the volume control of the melt pool, carried out by modulating the laser power of a continuous (cw)-coupled solid-state laser in fiber. During this process, regular surface structures are generated by the redistribution of the material in the molten state. The height of the resulting structure is linearly dependent on the amplitude of the laser power and can be adjusted from a few microns up to several hundred microns.

In practice, the maximum laser output power of this system is approximately 400 W and can be focused on laser beam diameters in the range from 150 to 800 µm. A thin surface layer (< 100 µm) is melted and subsequently solidifies. The direction of solidification follows the surface of the melt pool. With constant laser power, the surface of the melt pool is approximately flat and no texture appears. As the laser power increases, the volume of the melt pool increases and the surface of the melt pool swells outward due to the change in density from solid to liquid as well as to the increased volume of the melt. Solidification follows the swollen surface and structuring is achieved. As the laser power decreases, the process works the opposite way. Thus, with a modulation of the laser power during the remelting of a thin surface layer, structuring can be achieved. The Wave Shape process compared to the laser polishing processes allows to have periodic structures as desired.

2.4 Structuring by recoil pressure

Similar to Wave Shape surface structuring by laser remelting, but more recently introduced is the surface structuring by vapor pressure [89]. It represents a new hybrid process in which the structuring takes place without significant loss of material but mainly through redistribution of the material in the molten state. A combination of pulsed and cw laser radiation is used for structuring, in which both laser beams are used simultaneously. With the continuous laser beam, a melt pool of near constant volume is generated at defined laser power and scanning speeds. A small amount of material is locally evaporated from the melting pool by pulsed laser radiation (Fig. 5d).

For surface rippling during laser polishing, changes in the volume of the melt pool and the surface of the melt pool cause the formation of structures over the surface. Due to the additional energy introduced into the melt pool by a pulsed laser beam, the evaporation of a small amount of material creates a vapor pressure that deforms the surface of the melt pool. This deformation of the surface of the melt pool leads to a change in the solidification angle of the melt pool. Solidification of the molten material usually occurs along the solidification angle and therefore along the surface of the melt pool. Therefore, the angle of solidification Θ determines the direction of solidification. By changing the solidification angle, it is possible to obtain the texturization of a surface almost without material removal. Compared to the Wave Shape process, it should be possible to change the solidification angle more quickly by local evaporation of the material on the one hand and on the other to make possible greater changes in the solidification angle. Overall, the prospect is to be able to produce larger structures in a shorter time by controlling the melt pool solidification angle with volumes significantly less than one cubic millimeter.

As far as surface processing is concerned, laser technology is mainly used for the purpose of polishing (see Fig. 6a), to reduce roughness and improve the surface finish. An increasingly atypical use of technology has, however, made it possible to evolve towards further application areas, not of secondary importance, such as that of the "structuring of surfaces" (see Fig. 6b). After a first finishing using conventional technologies, in this specific case by sandblasting, laser polishing can also be selectively applied, combining the various process parameters in an appropriate way. By focusing the laser beam only in certain areas, it is possible to design a surface by creating grooves and particular surface textures as, for example, can be seen in Fig. 6c. In this way, a contrast is obtained between the more opaque areas (obtained by sandblasting) and the more glossy areas (obtained thanks to remelting).

3 General applications of laser polishing technologies

The effect of the operating parameters on the quality of the laser polishing process has been studied by several researchers. The experimental works herein reported concern the applications of the laser polishing, with a specific focus on both macro-polishing and micro-polishing. The applications refer to polishing carried out on components achieved by conventional processes and by AM technologies.

Laser polishing is carried out on the surface of the workpiece, involving a specific area of the material, even relatively large. Together with the main process parameters, a scanning strategy for the area that will be affected by the polishing process must be chosen. This is because during laser processing, the temperature distribution changes rapidly during the quick movement of the energy beam. Therefore, high-temperature gradients could be caused by the high energy input delivered in very restricted area of the component, leading to high residual stresses and non-uniform local deformations. A shield gas is almost always used during processing to avoid surface oxidation of the component. The gas can flow directly to the surface of the component, or the process can be carried out inside a box in which there is a protective gas atmosphere.

Figure 7 shows the surface of a component during laser polishing that must be scanned according to the prescribed patterns in order to have a process that is as homogeneous as possible. In fact, knowing the width of the track (b), a specific scanning strategy must be

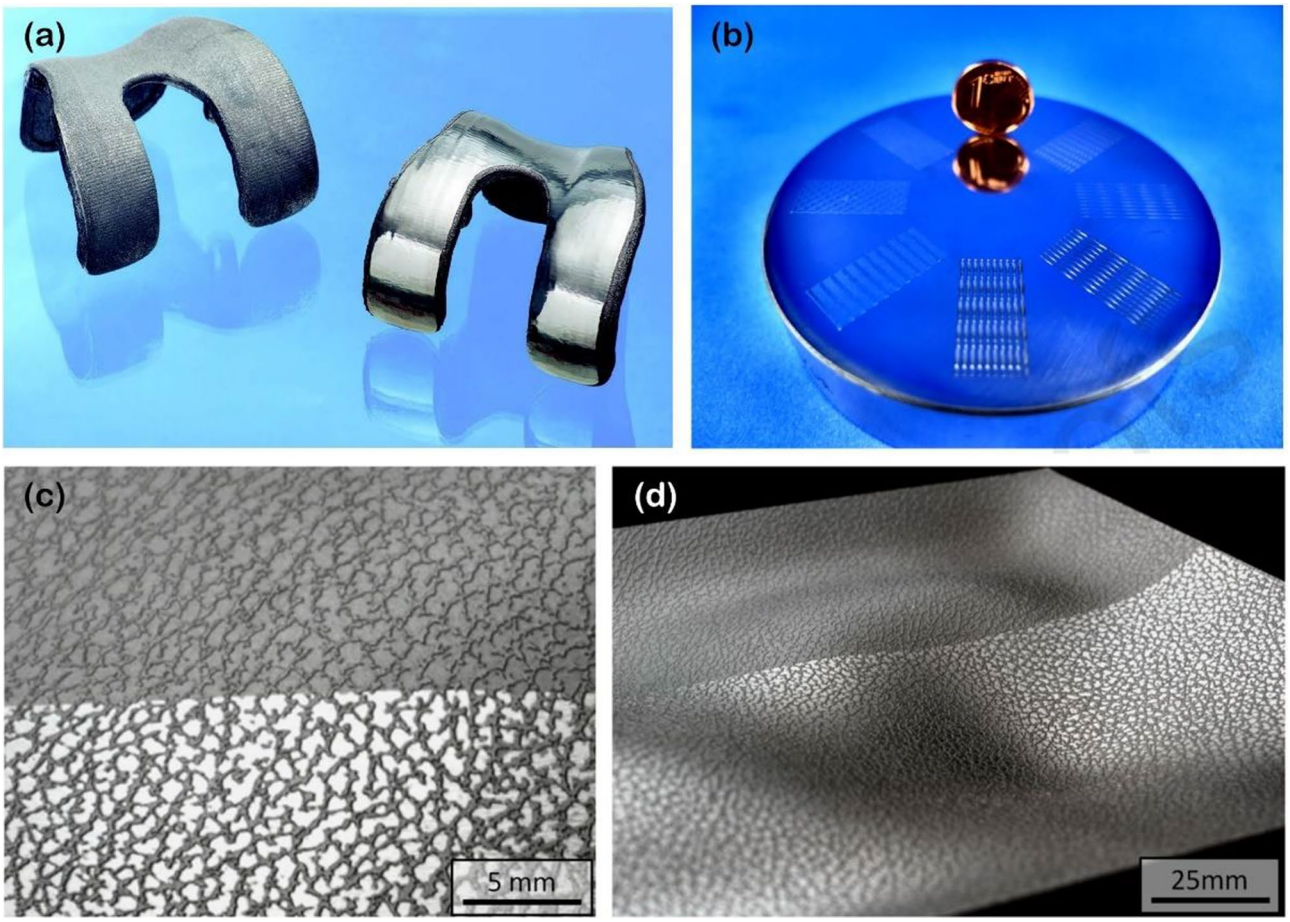

Fig. 6 (**a**) Unprocessed and laser polished knee joint, produced additively [91]; (**b**) different surface structures produced by laser wave shape process on Inconel 718 [92]; (**c**, **d**) photograph of a selectively polished free-form surface portion by laser [71, 72]

provided to process the entire area. Different types of scanning strategies were examined by Giorleo et al. [93], as highlighted in Fig. 8.

Taking the half circumference as a reference, it is possible to choose strategies with two superimposed lines of 90° (a), three lines (b), or have the laser beam follow an

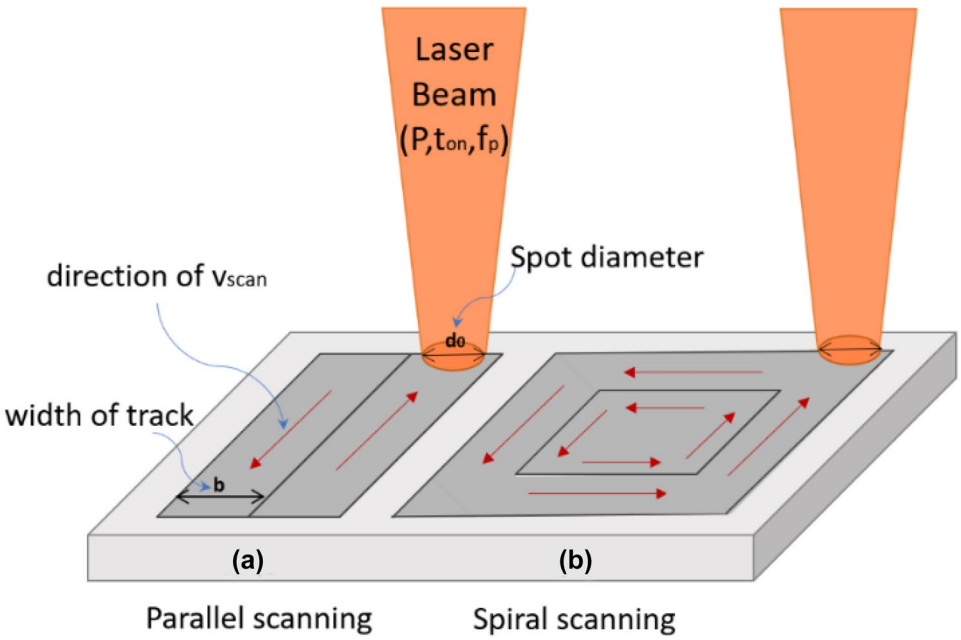

Fig. 7 Main scanning strategies in the laser processing path: (**a**) parallel scanning (**b**) spiral scanning

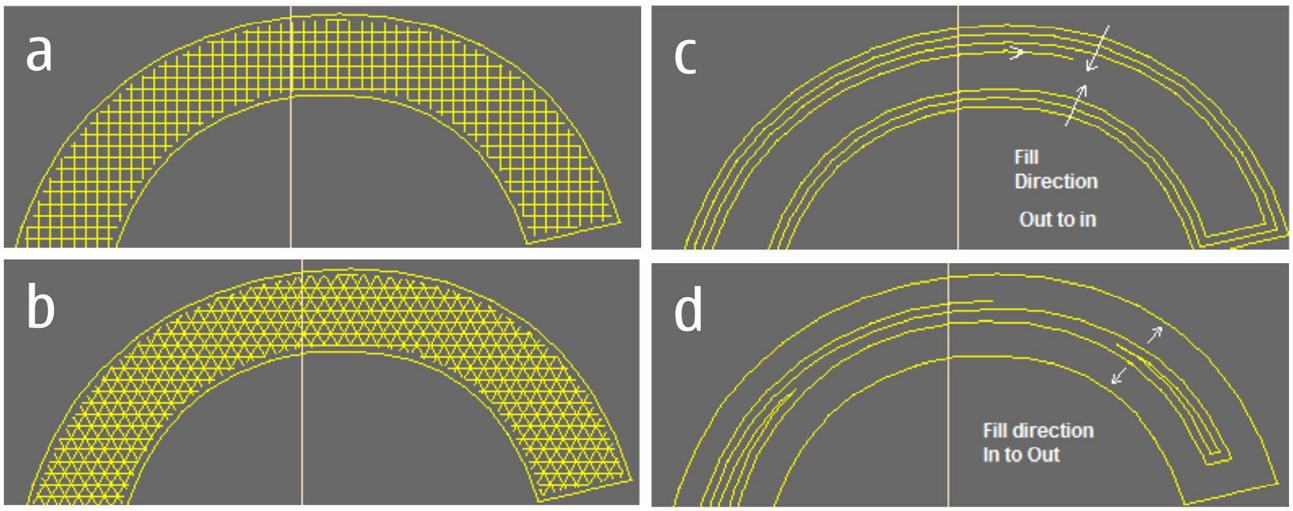

Fig. 8 Scanning strategies tested by Giorleo et al. [93] for the filling path: (**a**) two line, (**b**) three line, (**c**) out-to-in line, (**d**) in-to-out line

offset of the perimeter from the outside to the inside (c), or vice versa (d). One of the parameters that characterize the scanning strategy in both cases (micro and macro) is the hatch spacing, which is the distance between the centers of two adjacent traces. Comparing the processes of macro- and micro-polishing, being different the way in which the power is supplied to the material, the thermally altered zone will be of different sizes. In the first case, especially with the adoption of not too high speeds, there will be an interaction time that will allow the heat to reach a more considerable thickness of material. On the other hand, through the use of short laser pulses, the heat will not have time to disperse and, therefore, the thermally altered area of the workpiece will be smaller in size. Furthermore, by adopting a pulsed profile, since the molten area is smaller in size, at the same temperature, the irradiated material will take longer to cool down and, therefore, it will have a lower solidification speed, probably avoiding the formation of hard structures after laser processing.

In addition to the temporal distribution of the beam, also its spatial distribution is of fundamental importance for laser polishing. In processes in which the machining of more or less large surfaces is involved, the homogeneity of the machining is always necessary. For example, adopting a laser source characterized by a beam with a Gaussian power distribution and performing the processing with the zigzag scanning strategy shown in Fig. 8, there would be a non-uniformity in the trace amplitude. In the center, a good melting of the material would be obtained while in the sides, where the energy is minimal, material melting might not even take place. This problem can be solved by overlapping the tracks, choosing a smaller hatch spacing, but, in this way, the processing would require too much processing time. For this reason, flat top distributions of the power of the laser beam are preferred for laser polishing. This would allow to have the energy distributed in a more uniform way on the component during processing, with an increase in the overall effectiveness of the post-treatment.

Temmler et al. [71, 72] have thoroughly analyzed the laser polishing process on carbon steel samples. The effect was studied in terms of average roughness measured by white light interferometry at two levels of magnification and by filtering the roughness maps based on a spatial wavelength (Fig. 9). The experimentation was carried out using a solid state Yb:YAG laser source with a maximum power of 550 W and using for the pulsed mode t_{on} ranging from 0.7 to 3.5 ms at high frequency (5–20 kHz). From the experimental results obtained, the choice of a continuous source or a pulsed source depends on the initial roughness and the chosen spatial wavelength λ. In fact, consistent reductions in surface roughness are obtained in the range $80 < \lambda < 1200$ µm by macro-laser polishing, while for $\lambda < 80$ µm by micro-laser polishing. Furthermore, the authors have also focused on the combination of the two processes in order to obtain an improvement of the surface finish on all spatial wavelengths. Starting from an unmachined surface, they first subjected it to a scan made with a continuous source, obtaining a significant reduction in roughness (70–90% of the initial roughness) thanks to the molten material which redistributes itself in a more homogeneous way. Subsequently, they reprocessed the same surface with a pulsed laser, obtaining a further improvement in the surface finish (further reduction of micro- and meso-roughness up to 50%). A combined treatment of cw and pulsed laser radiation therefore makes it possible to create a double-gloss surface.

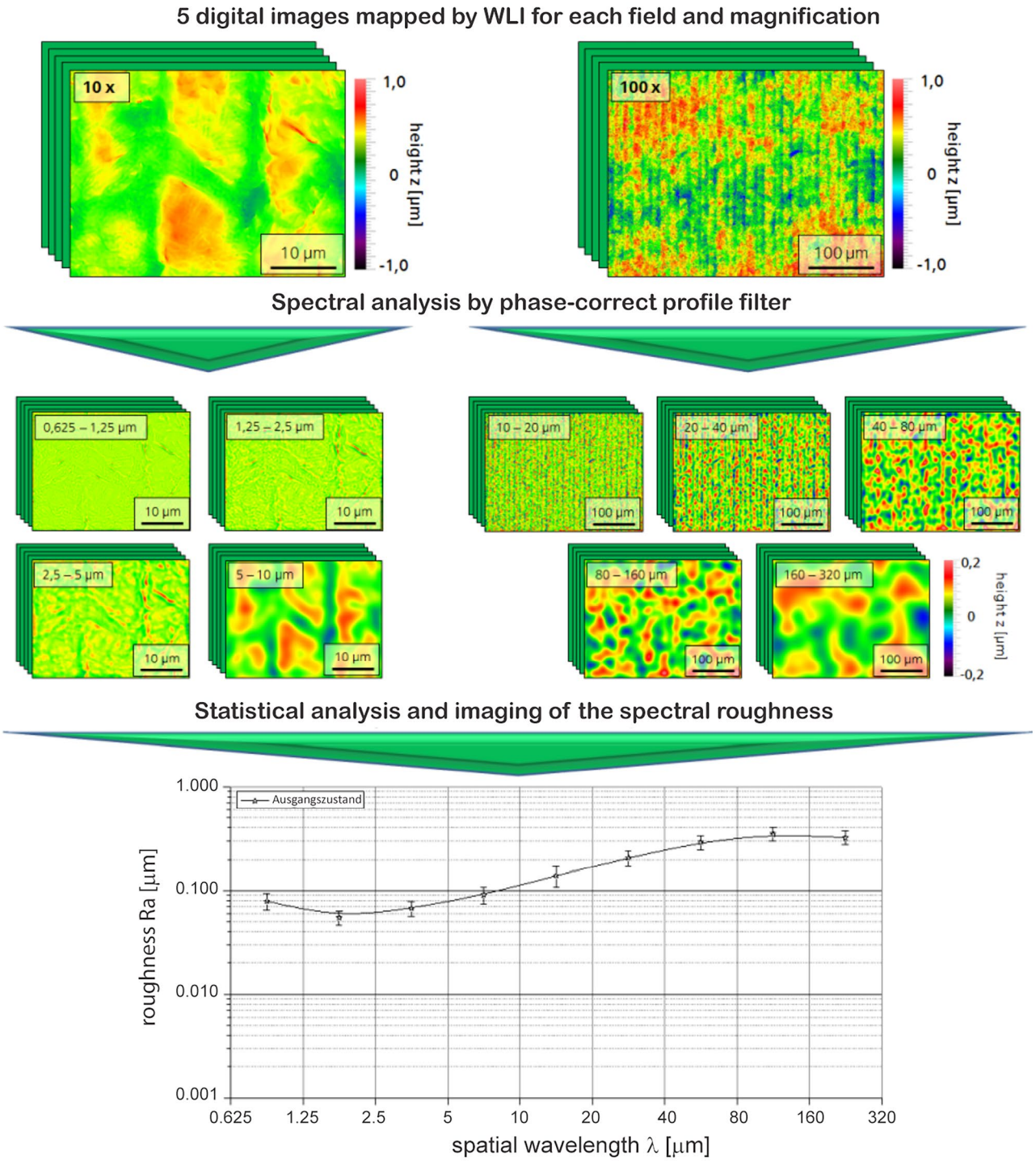

Fig. 9 (**a**) Schematic of process principle and main procedural parameters for laser polishing. (**b**) Schematic for spectral analysis of surfaces based on different WLI mappings [71, 72]

In Giorleo et al. [93], laser polishing on titanium alloy (grade 2) sheets was analyzed. Referring the previous scanning strategies in Fig. 10, the authors focus their research on how the variation of process parameters (scanning speed and assist gas) can affect the average roughness R_a in the finishing process. A pulsed Nd:YVO_4 source with a maximum power of 8 W was used in the experimental plan and particular emphasis was posed on the shielding gas. After the process, the difference between the initial and final roughness is evaluated and reported in Fig. 10a,

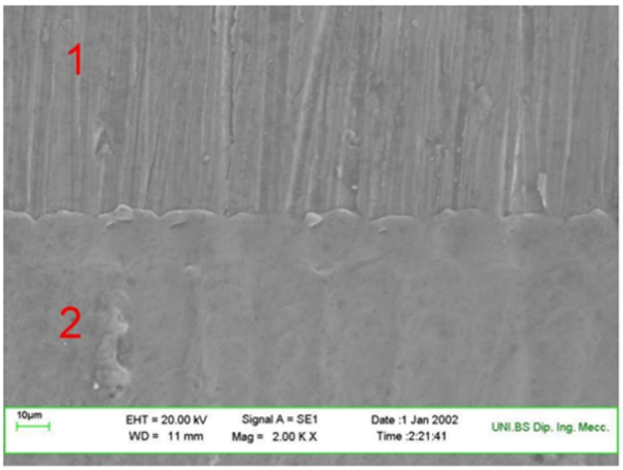

(a)

Laser Path	Gas [bar]	R_{a_med} [μm]	σ
BASE MATERIAL		0.58	0.082
	0	0.42	0.069
TWO LINE (2.371 s)	5	0.49	0.040
	10	0.53	0.058
	0	0.44	0.046
THREE LINE (3.557 s)	5	0.50	0.045
	10	0.54	0.049
	0	0.47	0.046
IN-TO-OUT (1.357 s)	5	0.49	0.068
	10	0.55	0.057
	0	0.47	0.076
OUT-TO-IN (1.404 s)	5	0.51	0.084
	10	0.58	0.065

(b)

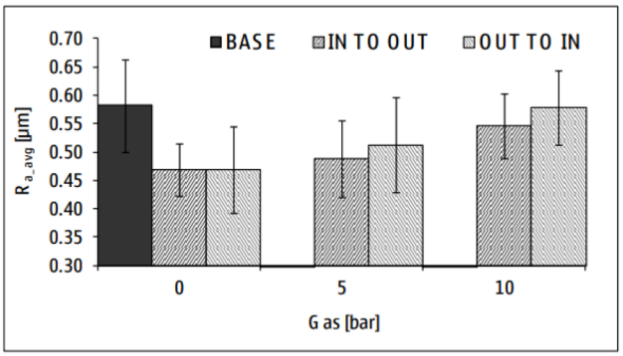

(c)

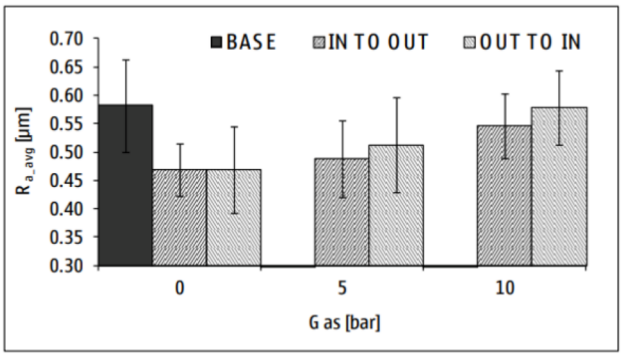

(d)

Fig. 10 Laser polishing on titanium grade 2 sheet: (**a**) comparison between raw surface (1) and laser polished surface (2); (**b**) improvements in average roughness and quantitative analysis; (**c**) medium average roughness evaluated from the two and three line campaign; (**d**) medium average roughness evaluated from the in-to-out and out-to-in line campaign [93]

d. The presence of shielding gas is necessary, since in addition to avoiding annoying oxidations, it also allows drops of molten material to be pushed out of the work area so that they do not damage the machined surface. However, too high gas flow rates (higher than 5 bar) reduce the quality of the processing, generating a turbulent motion of the molten metal which, as it moves, creates unwanted valleys. Too high speed (> 7 m/s) causes morphologies to be generated on the surface that "copy" the various pulses of the laser during processing. Set the working frequency, a higher speed causes the pulses are more spaced each other. In general, improvements are achieved with relatively low gas flow rates (5 bar) and low scan rates (5.5 m/s) as shown in Fig. 10c, d. The machining time for the optimized parameters was also calculated (Fig. 10b), and this turns out to be 4 s for an area of 5×5 mm^2.

Zhou et al. studied the behavior of laser polishing on Ti6Al4V titanium alloy, observing reductions of up to 90% in surface roughness and focused on the effect that the thermal cycle generates on the surface being polished. The rapid cooling can increase the surface hardness even by 25%, but, at the same time, an improvement is obtained in terms of the corrosion resistance of the surface. The experimentation conducted by Zhou et al. [21] is applied to hot rolled samples fabricated by a front milling process with which a startingroughness of about 7.3 μm is achieved. The laser equipment, on the other hand, is a continuous fiber source that provides a maximum power of 250 W. During the experimental tests, the laser beam was defocused to obtain a larger spot.

Kumstel and Kirsch [70] have also investigated titanium alloys. In particular, they have analyzed the effect of polishing by laser radiation (macro-polishing) on both titanium and nickel alloys, commonly used in aerospace (Ti6Al4V and Inconel 718). A continuous beam laser source was used for the experimentation, although in most of the researches on these alloys, a process of micro-polishing with pulsed sources is carried out. First, the dependence of the final roughness by the laser beam diameter is evaluated. The lower roughness is obtainable by operating with the smallest

diameters. For example, by operating on a turned profile with initial roughness $R_a = 1$ µm, values of $R_a = 0.15$ em can be obtained by operating with a diameter of 250 µm. The choice of the beam diameter, however, depends on the initial state of the surface, i.e., on how far the traces left by the turning or milling operations are. Once the spot diameter has been fixed, the influence of the other process parameters is then evaluated. For the titanium alloy, the rapid solidification gives rise to the formation of a hard micro-structure, of the martensitic type, and gives the formation of a thermally altered zone of comparable extension. In particular, the resulting hardness is maximum on the surface and decreases until reaching the non-thermally altered material which has the starting hardness of the alloy. The hardness in the remelted zone does not depend on the initial hardness of the alloy.

In Temmler et al. [68], the influence of the duration of a single pulse and frequency in the process of micro-polishing of AISI 410 stainless steel has been analyzed, operating with a Nd:YAG laser source and using pulse of variable durations in the range of 10 to 220 ns and frequencies in the range of 20 to 240 kHz. Once polished, an AISI 410 surface steel free from defects such as cracks or surface imperfections can be obtained. The best finishes are obtained by combining the parameters of pulse duration and frequency in a proportional way, i.e., avoiding combinations of short pulse and high frequency, thus ensuring that the pulses reach the material only when it is in a solid state. The level of gloss of the surface increases as a function of the decrease in micro-roughness, making the material particularly interesting for decorative design applications.

Miller et al. [94] focused on the effects that the laser and scanner control parameters have on the formation of surfaces with better quality, operating on ground specimens in tool steel (H13). In particular, by a CW source (YLR-500 fiber IPG Photonics) fitted with a plane field lens, they have analyzed the influence of the delay in laser switch on/switch off parameter. They varied these parameters along with the beam power, while leaving unchanged the scanning speed at 100 mm/s. Using an appropriate control system, the authors demonstrated that it is possible to create power and speed ramps that improve the single trace left on the material, making it more uniform. The non-uniformity occurs in the areas in which there is a transient regime of the beam power and scanning speed. Therefore, the effect of acceleration and deceleration during laser processing plays a crucial role in having a trace of constant size. Using different linear ramps of the beam power and scanning speed, dissimilar results are obtained. In particular, the best result is the last one represented in Fig. 11, in which a new strategy is used. As seen from the speed and power trends, the slope of the straight lines and also the start and end point appear to be different in the three scenarios. In the optimized strategy, the speed ramp has a lower slope than that of the power. It starts in advance and ends later, ensuring a perfect synchronization of the time in which the two parameters are set at constant values. When the speed has reached an almost constant value, the laser beam emits the power almost instantaneously since the slope of the power ramp is much greater. In this way, the handling system will be at a constant speed and the power delivered almost instantaneously by the beam will be constantly transported during processing.

De Giorgi et al. [95] analyzed the feasibility of the micro-laser polishing process on AISI 304 stainless steels for biomedical purposes. The experiments were conducted in three different atmospheres: ambient, argon, and nitrogen, and a large number of process parameters were tested. The equipment used consists of a Q-switched fiber laser source and a scanning head equipped with a f-theta lens with a focal length of 100 mm and a diameter of the beam of 39 µm. The initial roughness of the samples ($R_a = 85.3 \pm 2.8$ nm) was reduced under optimized conditions by approximately 50%. The optimized conditions are those achieved in a protective atmosphere; therefore, it is always necessary to provide an environment in argon or nitrogen. Furthermore, with an increase in the energy level, the surface roughness is higher than the initial value, demonstrating that the laser micro-polishing can produce a greater surface roughness, despite the surface being visually brighter and smoother. In such case, it is necessary to defocus the laser beam so as to obtain lower irradiance.

In Ukar et al. [96], the application of the laser polishing process (macro) on components made of spheroidal cast iron for the construction of molds for foundries and molds for the automotive industry is presented. A macro-polishing process was used. At the microstructural level, spheroidal cast irons are characterized by the presence of graphite globules which have a melting temperature of approximately 3500 K. During the laser polishing process, the temperatures reached are approximately 1500 K. The graphite particles do not melt and tend to appear on the surface making it rough. In this regard, it is necessary to intervene by performing a decarburization of the surface. The laser equipment, in this specific case, was composed of a CW fiber source with a maximum power of 1 kW, the movement of the beam was carried out through a galvanometric system, and the focal spot was approximately 100 µm. After processing, no particular improvements in the surface finish were normally noticed due to the graphite particles. Accordingly, two different methods for triggering the reaction of decarburization are discussed. The first consists in performing the process in an oxygen atmosphere. Following the Ellingham diagram, at high temperatures, the reaction $2C + O_2 = 2CO$ is obtained, which involves the carbon contained in the graphite present on the surface of the sample. However, working with an oxygen atmosphere may be inconvenient due to the high

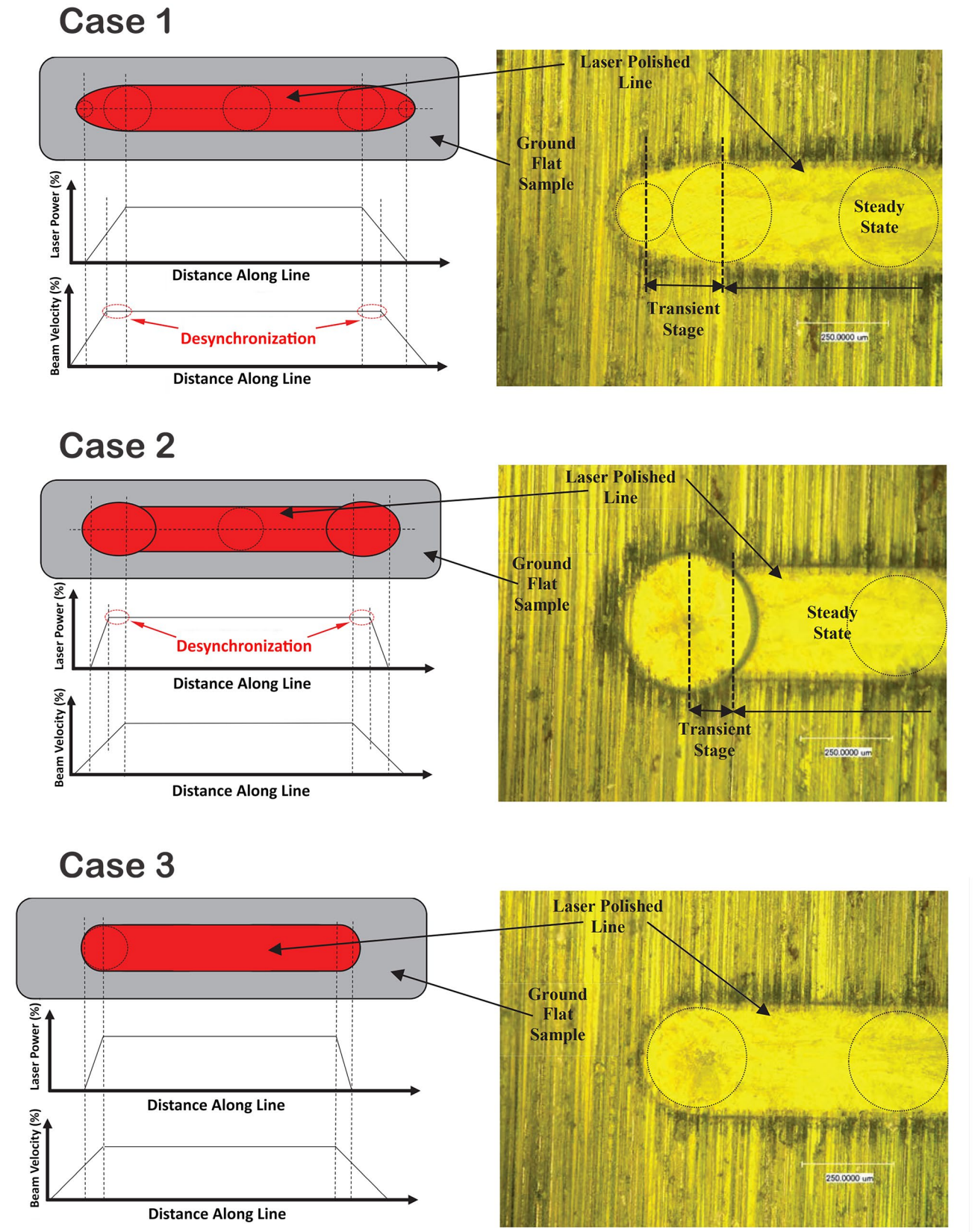

Fig. 11 Terminal geometry of a line generated under different combinations of laser power and beam velocity: case 1: laser speed gradient "ahead of" laser power gradient; case 2: laser power gradient "ahead of" laser speed gradient; case 3: laser speed gradient "in sync with" laser power gradient [94]

risk of combustion. The second method involved a carbon dioxide atmosphere, with the carbon being removed according to the following reaction: $C + CO_2 = 2CO$. In the latter method, preferable in terms of safety, it is necessary to ensure a correct filling of the sealed chamber as the carbon dioxide tends to accumulate in the lower part of the volume. The best results, with surface roughness reductions of up to 88%, are obtained using a power of 250 W and a speed of 100 mm/s, setting a hatch spacing equal to 50% of the track width. The average surface roughness has an $R_a = 0.5$ µm and a hardened layer of 350 microns thick, a favorable effect for increasing wear resistance.

In Nüsser et al. [67], the influence of the spatial distribution of irradiance in the laser micro-polishing process is evaluated. The distributions being compared are the "quasi" Gaussian and the top-hat ones. In this work, the geometry of the focal spot of the beam is also studied. In fact, both the Gaussian distribution and the top hat are compared with a circular and rectangular spot. The process is applied to a tool steel (1.2343). Two different laser sources are used for the experimentation, and both can be operated in all the configurations of interest. The best spatial distribution of irradiance is the top-hat one with a circular geometry. Nusser et al. presented a technology different from the previous ones [66], in which the micro-laser polishing process is carried out with the aid of a second laser beam (dual-beam technology). The second laser beam was used to pre-heat the surface. The materials tested were two: a X38CrMoV5-1 martensitic steel for tool and a Ti6Al4V titanium alloy. In both cases, the starting surface was obtained by turning. As far as the steel is concerned, the surface was subsequently remelted in CW.

The two laser beams were simultaneously moved according to the scheme shown in Fig. 12a. The beam delivered in continuous mode precedes the one delivered in pulsed mode, going to pre-heat the surface without melting the material. A fiber-coupled disk laser in cw mode is used for pre-heating and a fiber-coupled rod laser for polishing of the surface. The disk laser is equipped with a fiber with a circular profile or with a fiber with a square profile resulting in a Gaussian-like and a top-hat intensity distribution, respectively as shown in Fig. 12b. An increase in the time elapsing between the end of a pulse and the complete resolidification of the pool of molten material causes a more homogeneous distribution of the melt. In addition, the irregularities due to the irradiance distribution of the beam can decrease as the lower amount of energy required by the pulsed laser source. Regarding the martensitic steels, pre-heating generates a higher temperature in the material adjacent to the melted zone and the solidification rate tends to decrease. However, the solidification rate remains sufficiently high to allow the formation of a martensitic structure. In addition, the heat penetrates deeper and more martensite is formed. For steels, however, there are no great advantages for surface roughness, the latter being in some cases even higher than the roughness of the surface polished with a single laser beam. Differently for the titanium alloy, using the dual-beam technology has

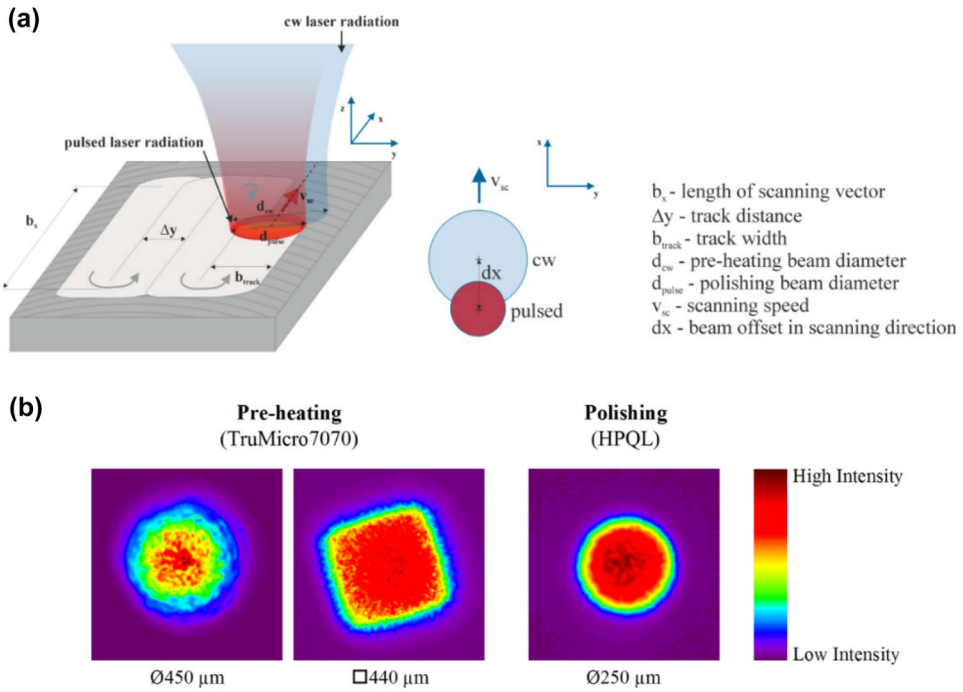

Fig. 12 Dual beam technology: (**a**) strategy for guiding the laser beams over the surface and top view of the two laser beams (**b**) intensity distribution of the laser radiation used in the investigation [66]

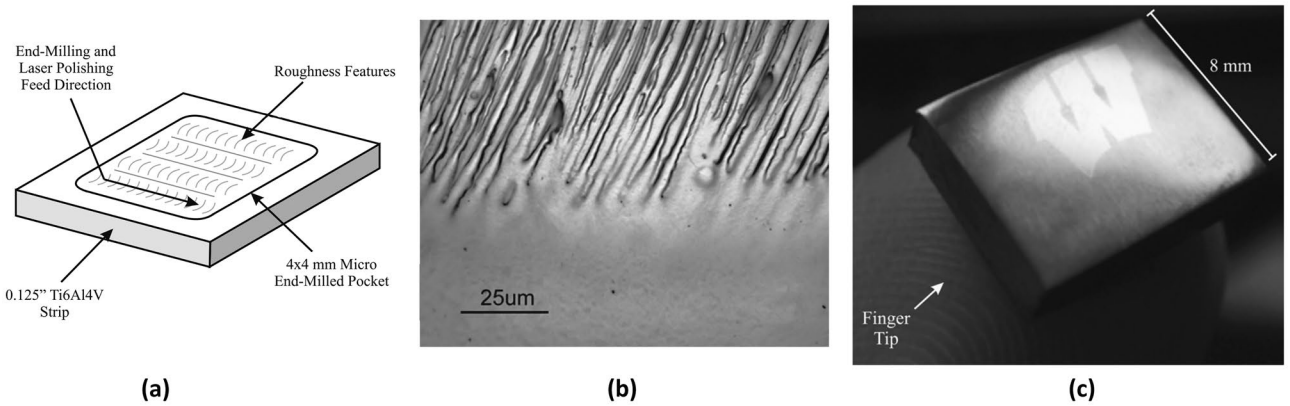

Fig. 13 Laser micro-polishing on the surface obtained by milling with argon shielding gas: (**a**) micro-end milled samples with laser path (**b**) the laser polished region is in the bottom half of the image (**c**) pattern polished on ground Ti6Al4V surface. The ''W'' is 5 mm in width [65, 97]

the same effects as using a pulsed laser with long pulses. A reduction of up to 36% of the roughness values was achieved on a meso-scale by increasing the power of the laser pre-heating.

In Perry et al. [97], attention was focused on the micro-polishing process applied to surfaces obtained through micro-milling, using the Ti6Al4V alloy. A pulsed (Q-switch) Nd:YAG laser with pulse durations of 600 ns at a fixed frequency of 4 kHz was used. The beam is moved by a scanning head in the direction parallel to the feed direction of the cutter. The laser beam hits the traces left by the processing as shown in Fig. 13.

From tests carried out in air, the polished surface has micro-cracks since, due to the high cooling rate, a thin and fragile layer of titanium oxide is formed. However, the problem is solved by processing the surface under inert gas. With the parameters mentioned in [65, 97], satisfactory reductions in R_a can be achieved, modifying its value from 0.206 to 0.070 µm. The authors show an 8×10 mm^2 sample of 0.125-in.-thick Ti6Al4V sheet that was ground to a matte finish using 800 grit silica carbide paper, and the smooth pattern, obtained using the PLµP process, engages a specific area on the surface, thus demonstrating the advantage of being able to operate selectively (Fig. 13c).

In Obeidi et al. [98], the efficiency of the macro-laser polishing process on AISI 316L austenitic stainless steel components produced by selective laser melting (SLM) is evaluated. A continuous mode laser source is used to polish cylindrical specimens which are rotated as shown in Fig. 14a.

Obeidi et al. [98] pointed out that the fabrication of curved or inclined surfaces leads to an increase in roughness due to the "stair case effect," while the fabrication

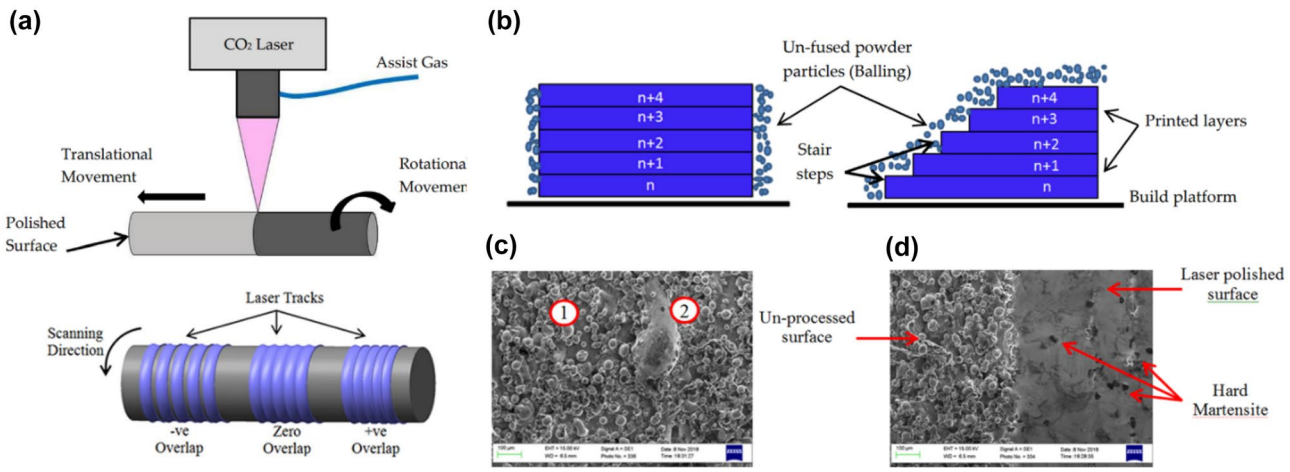

Fig. 14 Laser polishing of additive manufactured 316L stainless steel synthesized by SLM: (**a**) scheme of the experimental equipment with the three overlapping scenarios used for surface laser scanning passes (**b**) printing the vertical direction and curvature geometry (**c**) zones (1) and (2) show the balling effect and the partially melted and adhered neighboring particles (**d**) SEM image of AM 316L SST sample showing the same sample surface before (left) and after (right) laser polishing with 130 W, 30 rpm, and two passes repetition [98]

of vertical surfaces minimizes this effect (Fig. 14b). In this study, the samples were fabricated so that the cylinder axis is parallel to the layering directions. In this way, the step effect is minimized, but, in any case, the surface remains sprinkled with small dust particles that are only sintered but do not melt. So, the thermal energy that strikes the surface should only melt the non-fused particles that have remained adherent, while in the case of inclined or curved surfaces, a higher or more pass will be required. In Fig. 14c, zones (1) and (2), the rough surface of the as-built parts is shown, which is mainly caused by the sintering of the adjacent powder particles (i.e., balling effect), which is similar to micro-welding. The experiment conducted in Obeidi et al. [98] is divided into two different experimental plans. The first analyzes the effect of the beam power, the rotation speed of the sample, and the number of passes. In the second, instead, the optimized values of the beam power (110 W) and the number of passes (1) are fixed, while other parameters are varied, such as the overlap between the traces and the position along the z axis of the focal spot (Fig. 14a). The processed samples exhibit a wide range of roughness depending on the input parameters. The presence of the hard martensitic islands was observed on the re-solidified surface surrounded by the soft austenite (Fig. 14d). A reduction of the average roughness of about 25% was obtained, with R_a passing from 10.4 to 2.7 µm. It is necessary for this purpose to employ the lowest rotational speed (20 rpm), an overlap of traces of 20%, and focus the laser beam on the surface.

Gisario et al. [82] had also examined the possibility of performing a macro-laser polishing treatment on cylindrical surfaces in austenitic stainless steel (AISI 304). In this case, the starting surface is obtained by milling and the CW source used is a diode laser source (RofinSinar DL015) characterized, as known, by a larger spot. By scanning the milled surface with the highest powers and speeds, that is with 1300–1500 W and 120 rpm, respectively, very good and homogeneous finishing results can be obtained. Three different scenarios are examined for milling, with initial morphologies characterized by arithmetic roughness R_a as close as possible to 0.5, 1.0, and 1.5 mm. The laser post-processing demonstrates that it is possible to obtain asymptotic values of the roughness parameters, which do not depend on the initial roughness of the surface after the milling process but only on the operational settings. However, care must be taken to avoid surface overheating and melting of thicker substrate layers according to the surface overheating melting (SOM) mechanism.

Gisario et al. also use a diode laser source to process surfaces obtained by sintering [79, 83]. They investigate the possibility of smoothing the morphology of porous substrates consisting of spherical particles in sintered bronze, also evaluating the influence of laser treatment in terms of hardness and scratch resistance. With the laser treatments, it is possible to obtain a significant improvement in roughness parameters (see Fig. 15). To reduce the average roughness R_a by up to 70%, laser treatments must be performed at the highest powers and low interaction times. In particular, the power at which the laser polishing treatment can be considered effective is greater than 1350 W and the interaction times must be less than 0.5 s. Higher power is required due to the larger focal spot characteristic of a diode laser source. The improvement of the surface roughness is based, in this case, on the melting and resolidification process, which involves about two layers of micrometric spheres of 125 µm in diameter. The roughness profiles evolve from the concave-convex starting profile typical of the agglomeration of microspheres to the smoother and more uniform profile after high-power laser treatment. It is possible to obtain, at the same time, a sealing effect of the surface porosity of the sintered material, but it is necessary to estimate a reduction in the thickness of the sintered substrate of about 200 µm (i.e., 1/40 of the initial thickness).

4 Applications of laser polishing in AM technologies

In the last decade, laser additive manufacturing technology has undergone rapid expansion and can be considered a mature technology in several fields such as the aeronautical or aerospace [99–101] and the biomedical industrial segments [102, 103]. This is for the sometimes unique possibility of producing components with complex and highly customizable geometry in even shorter times than those allowed by the traditional fabrication processes. Indeed, the problem of polishing the rough surfaces of the workpiece constitutes a salient aspect that needs to be urgently resolved [104]. An increasing number of researchers is paying more and more attention to the application of laser polishing on workpiece fabricated by laser additive manufacturing as in addition to the advantage of exploiting the same technology,polishing using laser sources can concurrently improve the surface roughness of many manufactured parts and customize their morphological and thermo-mechanical properties [105–107].

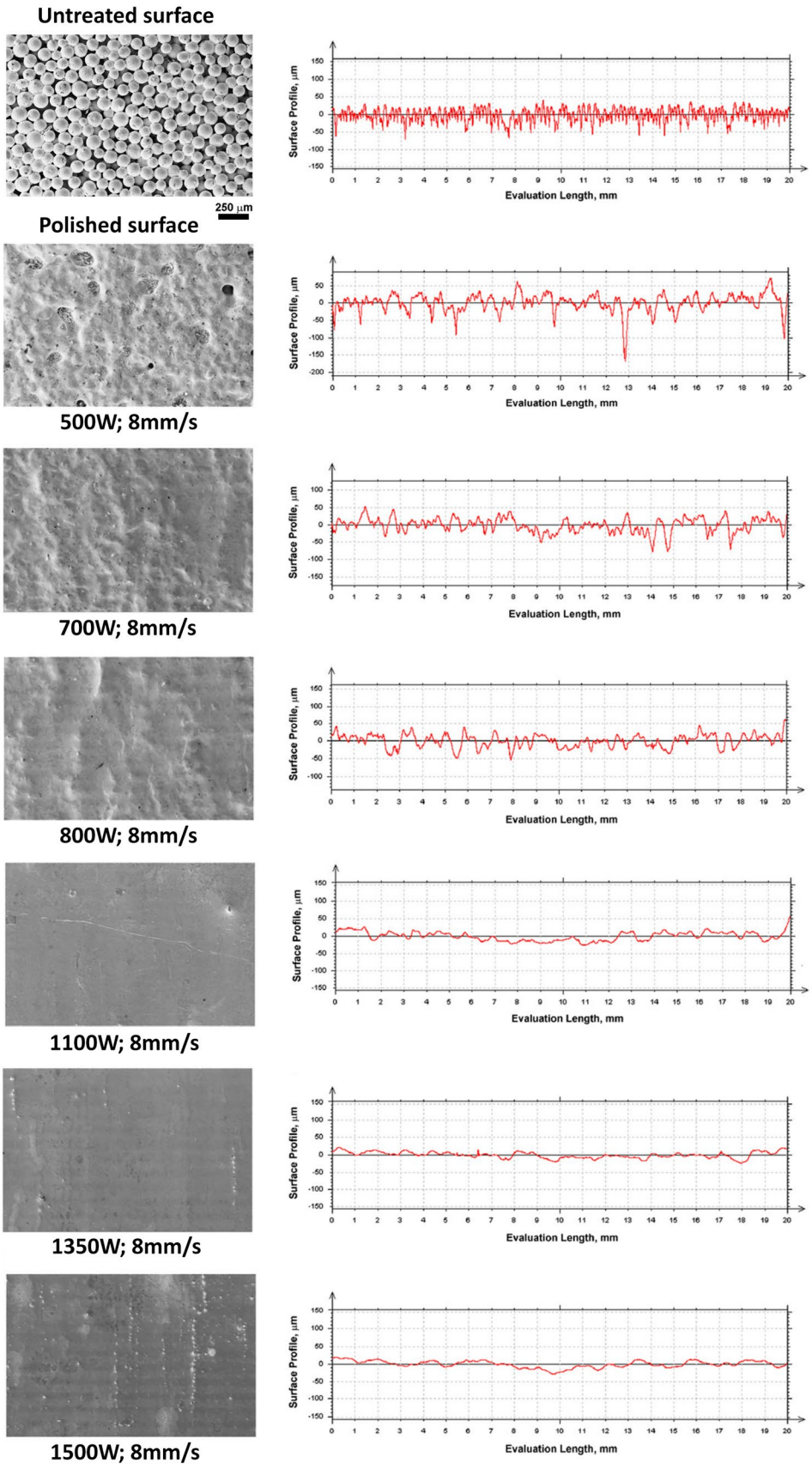

Fig. 15 Laser polishing of sintered bronze by cw high-power diode laser: SEM images and roughness profiles of laser untreated and treated surfaces at different levels of laser power with a scan speed of 8 mm/s [82]

In particular, Zhihao et al. [108] have investigated the possibility of performing the surface finishing by laser polishing of components in Inconel 718 superalloy manufactured by means of AM technology (Fig. 16). For the scope of the analysis, the authors have used a short pulse fiber laser of the order of nanoseconds. The IN718 samples were subjected to laser polishing treatment starting from an initial roughness that ranged between 7 and 8 µm. To avoid thermal oxidation, the polishing process was carried out in an argon atmosphere and the main process parameters were investigated keeping the power of the beam constant. Zhihao et al. [108] have shown that the surfaces produced via SLM, after the laser polishing process, show a significant reduction of R_a and R_z. In particular, the R_a shows a decrease from 7.5 to 0.1 µm while R_z from 31 to approximately 0.6 µm. From the metallurgical point of view, the superalloy IN718 shows a reduction in the dimension of the crystallites due to the rapid cooling and an increase in the precipitation of the phase in the layer that is remelted. The phase is a metastable precipitate of Ni_3Nb which has a body-centered tetragonal structure. It is one of the main phases that strengthen the Inconel 718 alloy [109]. For prolonged heat treatments or high-temperature heat treatments, it evolves into the δ phase, but being very rapid the cooling that occurs during the laser polishing treatment, the δ phase precipitates as γ'' phase. This phase precipitates into the remelted layer in the form of nanosized disks. The surface hardness is increased from 345 to 440 HV. In addition, wear resistance is also tested in the research. The friction coefficient decreases significantly. Therefore, wear resistance properties of the material can consequently be improved by the laser polishing process.

Chen et al. [110] analyzed the surface characteristics and the corrosion behavior of an AISI 316L stainless steel processed by power bed fusion and subsequently polished by means of a source (SPI Lasers) which operates in continuous mode. All the tests were carried out with the same power equal to $P = 50$ W, with a beam diameter equal to 200 µm that is obtained by defocusing the beam and an overlap of the traces fixed at 80%. As a result, the parameters that have been changed are the number of passes, the scan speed, and the energy density surface Es calculated as follows:

$$E_s = \frac{P}{DV_s}\left[\frac{J}{mm^2}\right] \quad (1)$$

Most of the defects that are present on the surface of the AISI 316L steel samples manufactured by selective laser melting are the residues of metal powders that are partially melted and the sintered powders that are not melted, still visible in Fig. 17. By observing the processed areas, it is possible to observe that they are smoother and also appear brighter (i.e., less scattering of the incident light radiation). In particular, Fig. 17a shows the effect of the process with a single pass, while in Fig. 17c, three passes have been made. When making a single pass, there are still some irregularities on the surface. The effect of the sweep speed can be observed by comparing Fig. 17a, b, both performed with a single pass but at speeds of 100 and 200 mm/s, respectively. In particular, it is noted that by operating at high speeds (Fig. 17b), the traces left by the laser beam are visible due to a shorter interaction time with the material. In Fig. 18, the cross section of the sample is represented in which the pools of molten material are noted. Processing the top surface shows that the layer is remelted, but changes are also observed in the pools of molten material below. The surface roughness has been reduced by 92.6% by operating with the following optimized parameters: 100 mm/s and 3 passes. The corrosion resistance of the sample in HCl solution is increased thanks to the less rough surface, because the polished samples offer greater resistance to the passage of electrons.

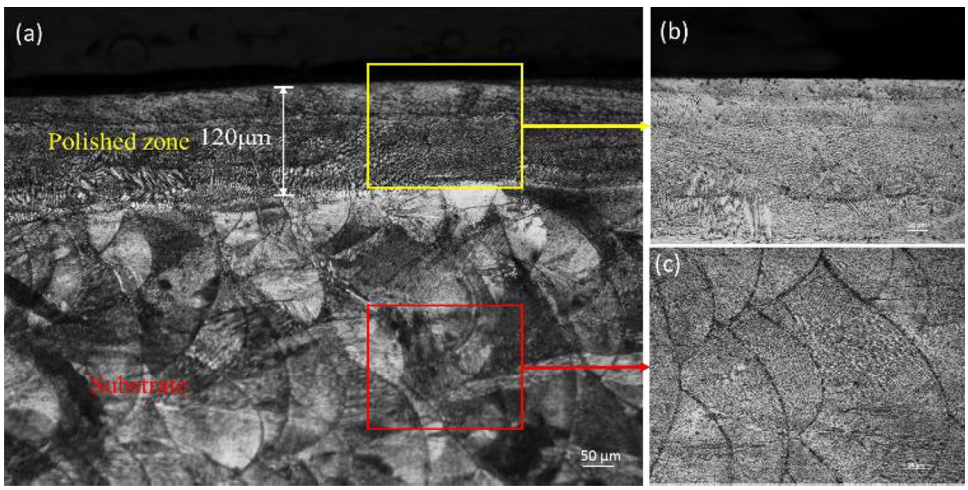

Fig. 16 Surface finishing by laser polishing of components in Inconel 718 superalloy manufactured by means of AM technology [108]

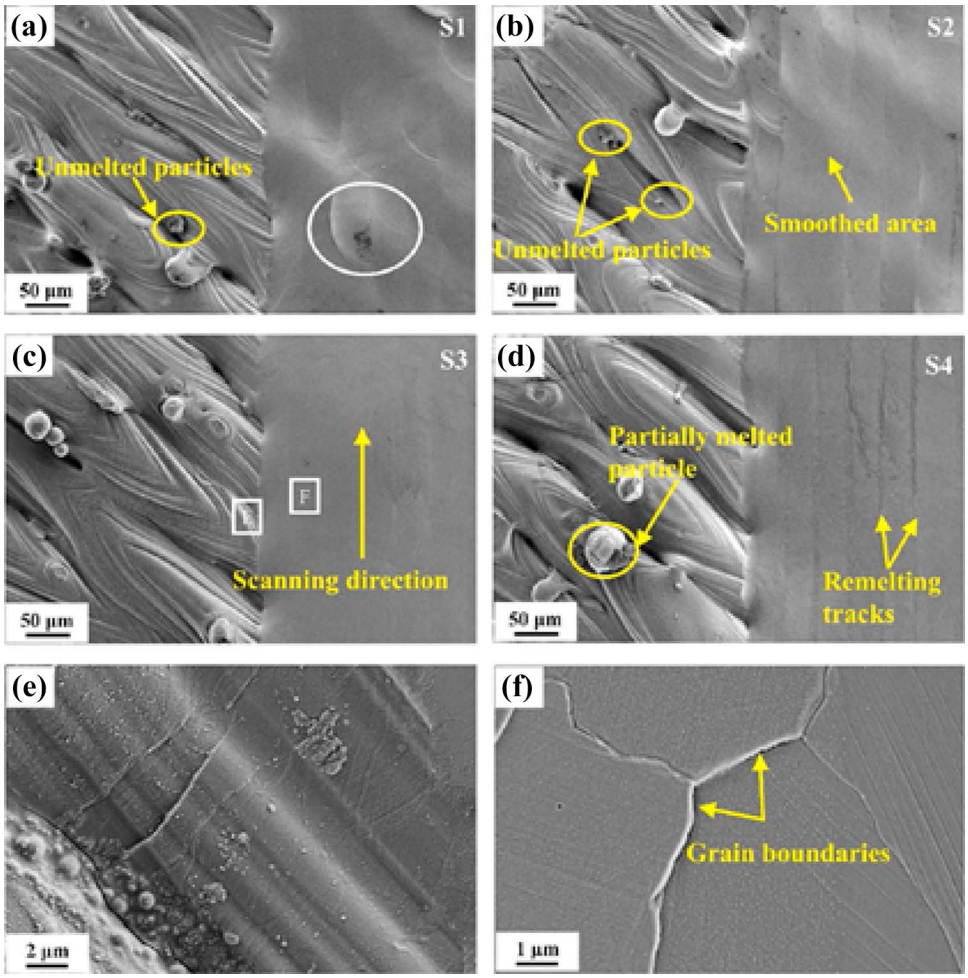

Fig. 17 Micrographs of the surface of the samples in AISI 316 L after laser treatment [110]

In dos Santos Solheid et al. [111], samples of maraging steel (18-Ni 300 grade) produced by SLM technology was subjected to laser polishing to observe difference in the use of a Nd:YAG Q-switch source (pulse duration 200 ns) in the continuous or pulsed mode. In particular, the impact of laser polishing processing was assessed by comparing the results obtained in terms of surface roughness and microstructure of the surfaces involved in the process. An appreciable reduction in surface roughness R_a was observed using an average power of 50 W, a scanning speed of 300 mm/s, and a hatch spacing of 25 µm when the laser source operates with a continuous wave. The roughness R_a of the upper and lateral surfaces after the same laser processing is very similar (generally less than 1 µm, with 0.6 µm being the lowest value), even if their initial roughness has a significant difference: 2.7 ± 0.6 µm on the upper surface and 6.4 ± 0.8 µm on the side surface.

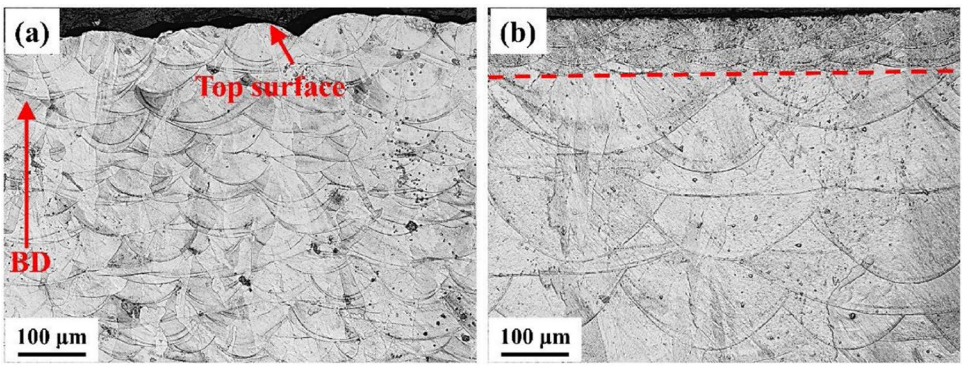

Fig. 18 Cross sections of the AISI 316 L samples after laser treatment [110]

Dos Santos Solheid et al. [111] noticed that, for small powers (5 W), there are no relevant effects on the surface (Fig. 19a). Increasing the power to about 20 W, they noticed the presence of cracks up to speeds of 100 mm/s (Fig. 19b). By further increasing the beam power at 25 W (Fig. 19c, the authors observed a marked removal of the material (laser ablation. Overall, the use of the continuous laser source has witnessed great potential in removing particles that remain adhered on the surface of the SLM component by vaporization, but the high temperatures reached always lead to undesired oxidation of the surface that must be avoided using an inert environment during processing. When processing affected larger areas, cracks were observed in all cases, even when they were not present in the single-track experiments; this is due to the number of repetitions, the recasting of the material resolidified, and higher average temperatures caused by laser scanning overlays. Operating instead with short pulses (ns, the authors have found the presence of pools of molten material that cause the formation of splatters on the surfaces (Fig. 19e). Those obtained with the combination of high beam powers and high frequencies are observable in Fig. 19e. On the contrary, those obtained by decreasing all the process parameters can be observed in Fig. 19d. These are visibly more stable melted pools ($P = 5$ W, $f = 30$ kHz, $v_s = 20$ mm/s). The AlSi10Mg alloy, typically used in additive manufacturing technologies, was analyzed by Schanz et al. [112]. The samples were manufactured also in this case by SLM choosing a layer thickness of 50 µm and conducting the treatment in a nitrogen atmosphere. The average starting roughness of the samples equal to 8.7 µm was reduced by applying the polishing process with a pulsed source with a maximum power of 4000 W. The focal spot diameter was of 430 µm, and the experimental setup involved the use of a 1-D scan head (Fig. 20a). Consequently, the laser beam oscillated in the direction indicated as transverse while the piece was moved in a feed direction orthogonal to the oscillation of the beam. The overlap of the traces was set by the authors on high values, in any case higher than 50%, by suitably varying the repetition frequency and the duration of the impulses together with the feeding speed of the component. A much higher power was used for the AlSi10Mg alloy, when compared to papers in which different materials are processed. This is partly due not only to the size of the focal spot, which in this case is large, but also to the fact that aluminum alloys absorb laser radiation inefficiently and are characterized by high thermal conductivity.

The energy that strikes the surface of the aluminum alloys is therefore partly reflected and partly dispersed in

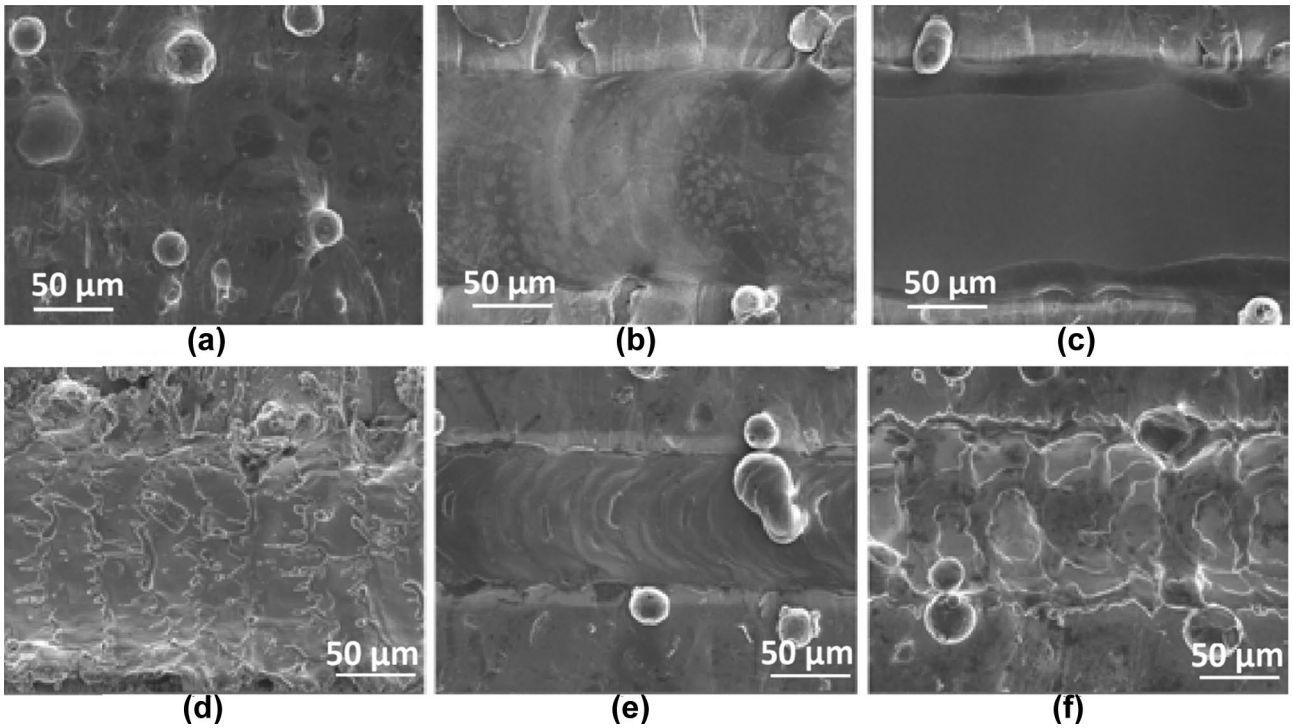

Fig. 19 Maraging steel surfaces subjected to CW laser polishing: (**a**) 5 W and 90 mm/s:no significant effect on the surface (**b**) 20 W and 20 mm/s: presence of cracks (**c**) 25 W and 90 mm/s: laser ablation. Maraging steel surfaces subjected to laser polishing PW (**d**) 25 W, 5 kHz, and 165 mm/s: excessive spatter and material removal (**e**) 5 W, 30 kHz, and 20 mm/s: more stable melt pools (**f**) 19 W, 60 kHz, and 90 mm/s: melt pool instabilities [111]

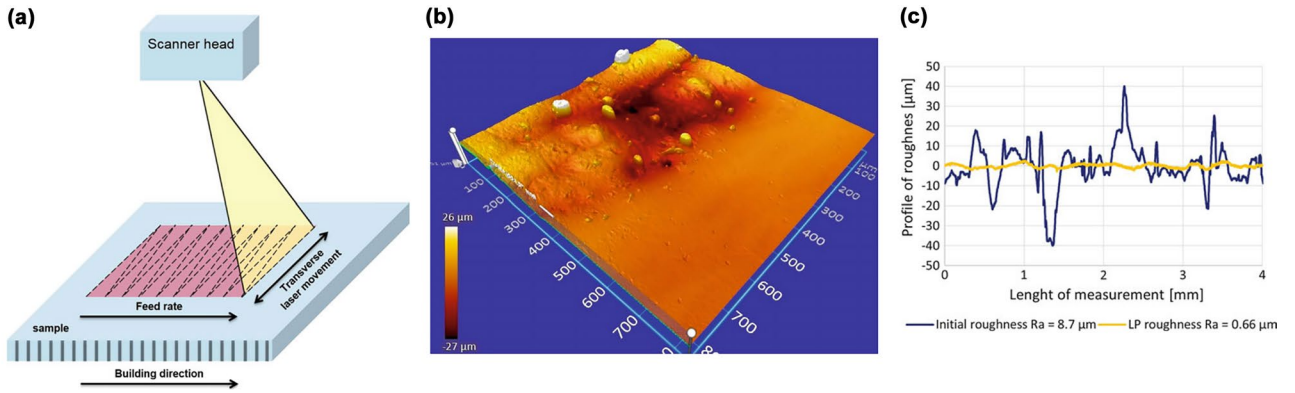

Fig. 20 (**a**) Schematically function principle of laser polishing with one-dimensional scanner head (**b**) transition area of the initial and polished surface, obtained with white light interferometer (**c**) comparison between initial and laser-polished surface [112]

the form of heat. Therefore, it is necessary to use a pulsed source with short pulses and high power so as not to allow time for the heat to disperse. The tests conducted have shown that with a power of 1700 W at high frequencies and with a feed rate of 40 mm/min, overlaps sufficiently high to avoid inhomogeneities on the surface can be achieved. Accordingly, it is possible to reduce the roughness up to 92%. However, the authors underline that the surface is not entirely polished, as some undulations and irregularities are still visible on the surface. Figure 20b, c show a comparison between the starting condition of the surface and the final result by evaluating the polishing process both by white light interferometer and by tactile measurements, respectively. An interesting study is that undertaken by Yung et al. [113] which have thought to apply laser polishing to metal components in CoCr with complex geometry manufactured by SLM in order to demonstrate that it may constitute a viable technology for the polishing of non-planar surfaces (Fig. 21(1)).

In most scientific works, tests are carried out on flat surfaces machined with different 2D scanning strategies. In this research, however, the attention is focused on a different method, the "layered laser polishing method." The interaction between the laser beam and a complex three-dimensional surface is different. It turns out to be much more complicated because it requires an optimization of the process parameters to obtain acceptable results. During the laser polishing process, the defocusing distance is a fundamental parameter and must absolutely remain constant throughout the process, so that the surface of the component always receives the same surface energy density. This condition is easily satisfied if the component being processed is planar and orthogonal to the laser beam but becomes more difficult if the surface has a complex geometry. To process complex geometries, it is therefore necessary to use a different technique. This layered laser polishing method is based on controlling the defocusing distance during laser polishing.

Yung et al. [113] have developed a simple geometric model for this purpose, which can also be conveniently adapted to work convex or inclined surfaces as well as any free-form surface. To control accurately the defocusing distance, the concave surface, observable in Fig. 21(2), must be divided into layers. The thickness of each layer must be smaller than the focal depth. Consequently, a different defocusing distance can be chosen for each layer, which remains constant on the single layer. In this way, it was possible to obtain reductions in the surface roughness up to 93% while operating on a complex surface geometry, a result similar to that achieved on planar surface. Starting from the initial roughness of about 4.23 µm, by laser polishing, a value of about 0.73 µm can be achieved. A pulsed fiber laser source is used, with the beam focused to a spot size of 50 µm and using an f-theta lens. The most important process parameters to perform the laser polishing are, therefore, the laser power (approximately 70 W) and the defocusing distance of 6 mm.

In another work, Wang et al. [114] (Fig. 22) have also analyzed the beneficial effect of laser polishing on the microstructural properties of the surface, with specific regard to corrosion resistance. It was observed that by effectively checking the hexagonal close packed (hcp) structures and the oxides formed on the outer layer, the samples in CoCr alloy produced by additive technology after laser polished reveal a greater resistance to corrosion, of about 30% compared to thermo-mechanically treated samples. This result is interesting for potential dental applications, such as dental implants, bridges, and

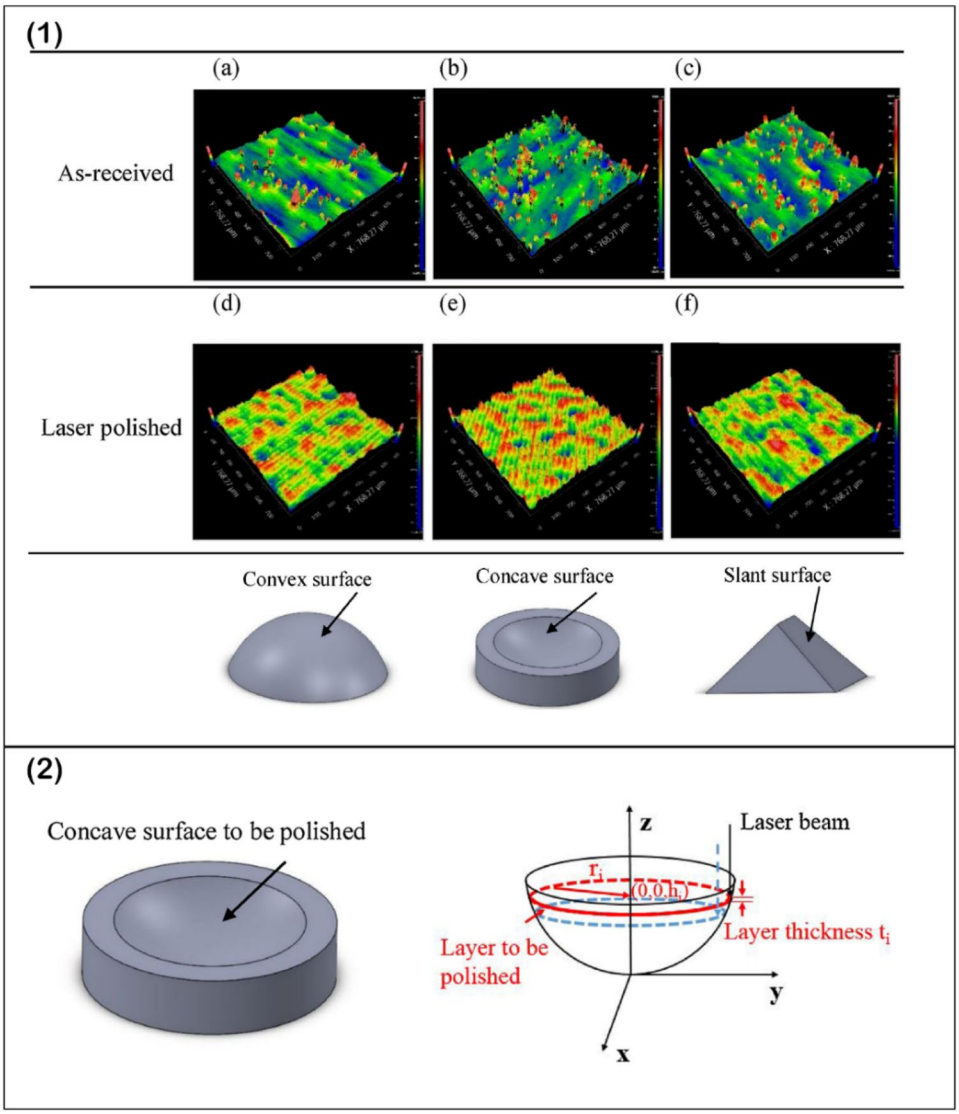

Fig. 21 (1) Surface morphology of samples with complex geometry before and after laser polishing. (**a**)–(**c**) As-received surface roughness of convex, concave, and slant surfaces, respectively. (**d**)–(**f**) Laser polished surface roughness of convex, concave, and slant surfaces, respectively. (2) Geometric model for laser polishing for the sample with a concave surface [113]

dentures for use in the oral environment. In fact, with the thermal action of the laser, it is possible to design a CoCr alloy with an anticorrosive protective layer and with unique properties. In addition, the surface microstructure in CoCr alloys processed by laser polishing is smooth and can contribute to increasing the resistance to build-up of bacterial plaque.

Dadbakhsh et al. [115] have examined how the laser polishing process can improve the surface finish of metal components in Inconel 718 manufactured by laser metal deposition (Fig. 23). The experimental results have shown that an effective improvement of the surface can be obtained through a correct modulation of the laser energy, which has proved to be the most influential factor capable of achieving a minimum and basically asymptotic level.

To calculate the optimal laser energy, it is necessary to intervene on the parameters of feeding speed, laser power and spot diameter according to Eq. (1), as already highlighted by some authors [80, 81] and, subsequently, taken up also by others [110]. Dadbakhsh et al. [115] show that, using a Trumpf DMD505 HQ CO_2 laser source with a beam diameter of 0.5 mm, it is possible to obtain maximum overall productivity by setting a laser power of 500 W, a speed of 800–850 mm/min and a 35% overlap. In this way, the surface roughness is effectively reduced by 80% with a final value of R_a below 2 µm (acceptable level for many applications, including aerospace ones). Dadbakhsh et al. [115] have always used Eq. (1) to calculate laser energy density, although they use a corrective factor of 6000 at numerator.

In Rosa et al. [116], an experimentation on the laser polishing of components manufactured by the LMD process, in AISI 316L steel, is reported. Also, in this case, the laser polishing experiments are carried out on the very same machine with which the component is manufactured.

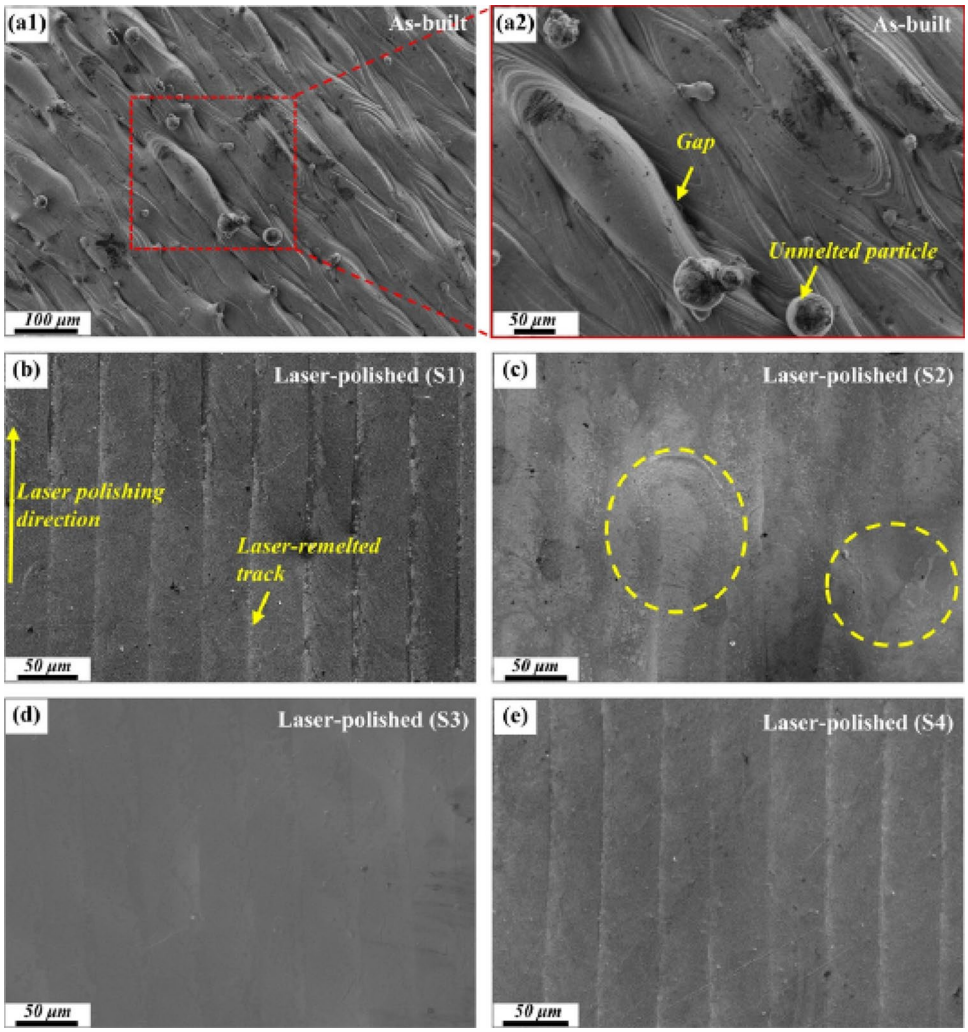

Fig. 22 Morphology of the top surface of CoCr alloy samples after laser polishing [114]

The machine is equipped with a fiber source of maximum power of 800 W. Surfaces are analyzed in terms of surface roughness S_a. Rosa et al. [116] showed that the best results (reduction of S_a from 21 to 0.79 µm) are obtained with a power of 210 W, a scan speed of 3000 mm/min, and an overlap of the tracks of 60% (Fig. 24). It has been

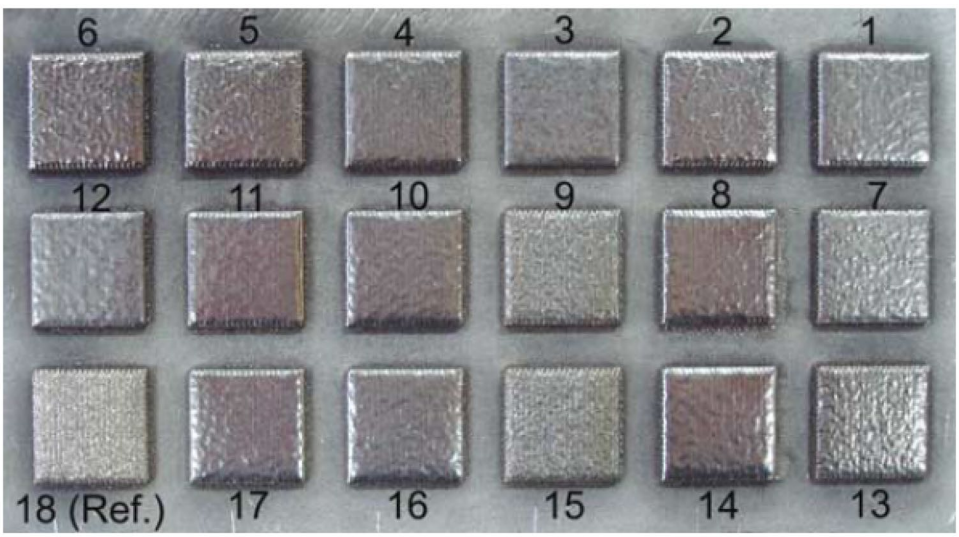

Fig. 23 Visual appearance of the surface finish after laser polishing of Inconel LMD parts [115]

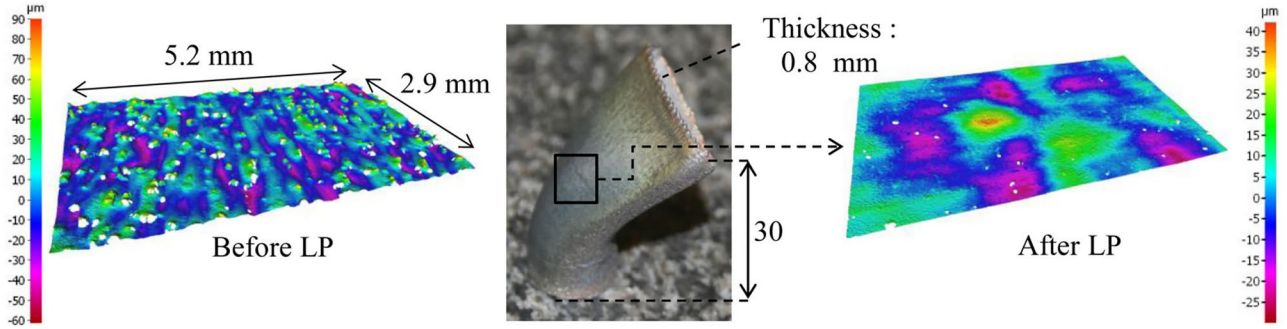

Fig. 24 Complex and thin part polished by laser [116]

deduced that by increasing the number of passes, there is further improvement of the surface and the elimination of the micro-cracks that are formed due to the first pass.

In Bhaduri et al. [117], the laser polishing process was applied to metal components obtained through the additive manufacturing technology developed by Digital Metal (https://digitalmetal.tech). Unlike the laser polishing processes that occur with the melting of metal powders, the technology developed by Digital Metal belongs to the "Binder Jetting" category. The single layer of metal powders is deposited as in SLM and EBM technologies and then is processed with a binder that "glues" the powders to form the single layer. The component is made with layer by layer technology and extracted from the machine to be subjected to a subsequent sintering process. This technology does not involve the melting of the material. Therefore, all the problems related to oxidation and the need to have a closed chamber with a protective atmosphere are avoided. In addition, the design of supporting structures is not necessary. However, the surface of the components needs post-processing. Bhaduri et al. [117] have optimized the laser polishing process on AISI 316L components manufactured with DM. The fiber laser source used delivers maximum beam power in pulsed mode and is equipped with a 3D scanning head. During the tests, the beam power and pulse duration were kept constant at 37.2 W and 220 ns, respectively.

By optimizing the process parameters, within a working chamber in which argon gas has been placed, a reduction of the surface roughness S_a of 94% was obtained. It has also been deduced that the intensity of the color is related to the amount of oxide formed and the depth of the oxidized layer. The use of an argon atmosphere significantly reduces this effect. Moreover, the estimated depth of the affected layer is shown in Fig. 25.

Ti6Al4V components produced via SLM for the aerospace industry were analyzed in Marimuthu et al. [118]. In this study, experimentation on laser polishing was carried out using a continuous beam mode. The focus is on the control of the process parameters and on the analysis of the dynamics of the pools of molten material generated by the laser beam. The dynamics of the pools of molten material

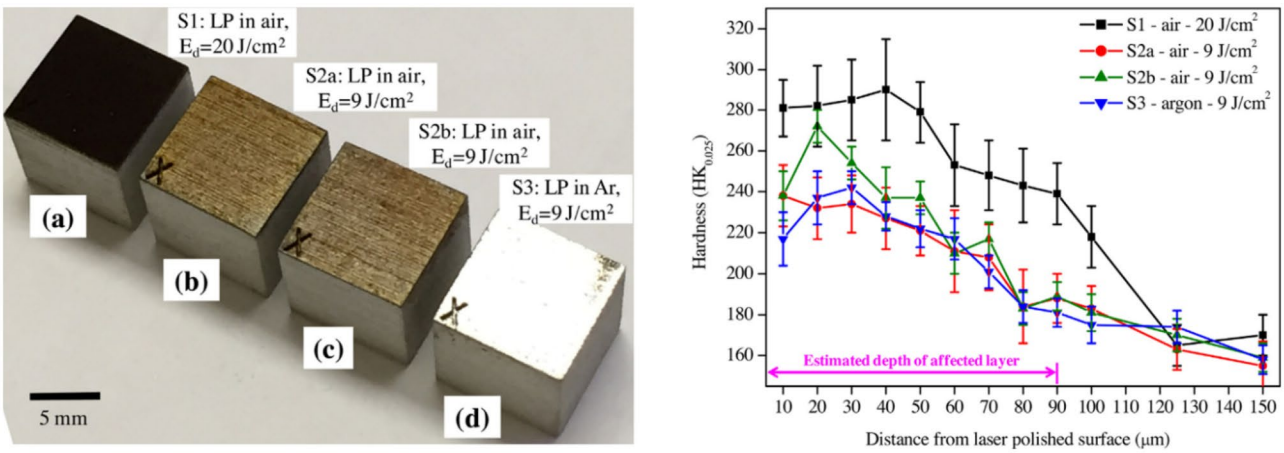

Fig. 25 Laser polishing AISI 316L: (on the left) images of SS cubes S1, S2a, and S2b laser polished in air at fluence of (**a**) 20 J/cm^2, (**b**, **c**) 9 J/cm^2, and (**d**) S3 in argon at 9 J/cm^2; (on the right) microhardness depth profiles of LP specimens in air and argon [117]

heavily influences the final result and a computational fluid dynamic (CFD) model to study the dynamics of the molten material was developed. The equipment used consists of a fiber laser source with a maximum power of 200 W and a laser spot of 500 mm. The spot size is obtained by maintaining a fixed distance between the component and the laser head. The surface roughness depends significantly on the velocity of the pool of molten material. The roughness is influenced by the power of the beam and the scanning speed. Increasing the laser power increases the speed of formation of the pool of molten material, with consequent formation of unwanted periodic streaks (Fig. 26). The usage of lower scanning speed allows, instead, to obtain broader polished traces, which constitute an advantage from the manufacturing point of view. An excessive input of thermal energy during the laser polishing process is however to be avoided as it can cause oxidation and carbonization of the surface.

Witkin et al. [119], operating on Inconel 625 metal alloy, were able to demonstrate that the laser polishing not always ensures a satisfactory improvement in respect of the fatigue behavior. It is known that the surface defects and the rough surfaces associated with the additive manufacturing degrade the high-cycle fatigue (HCF) properties of metals with respect to the traditional production technology. Improving the fatigue behavior of AM parts requires reducing their surface roughness at fatigue sensitive points that may not be accessible to standard machining operations. Being non-contact, laser finishing can provide greater accessibility without the need for extensive post-processing of the AM parts. The laser remelting seems to eliminate these types of surface characteristics. Nevertheless, the lack of improvement in the fatigue life can be considered linked to the presence of pores whose size varies arbitrarily. This determines the need to remelt

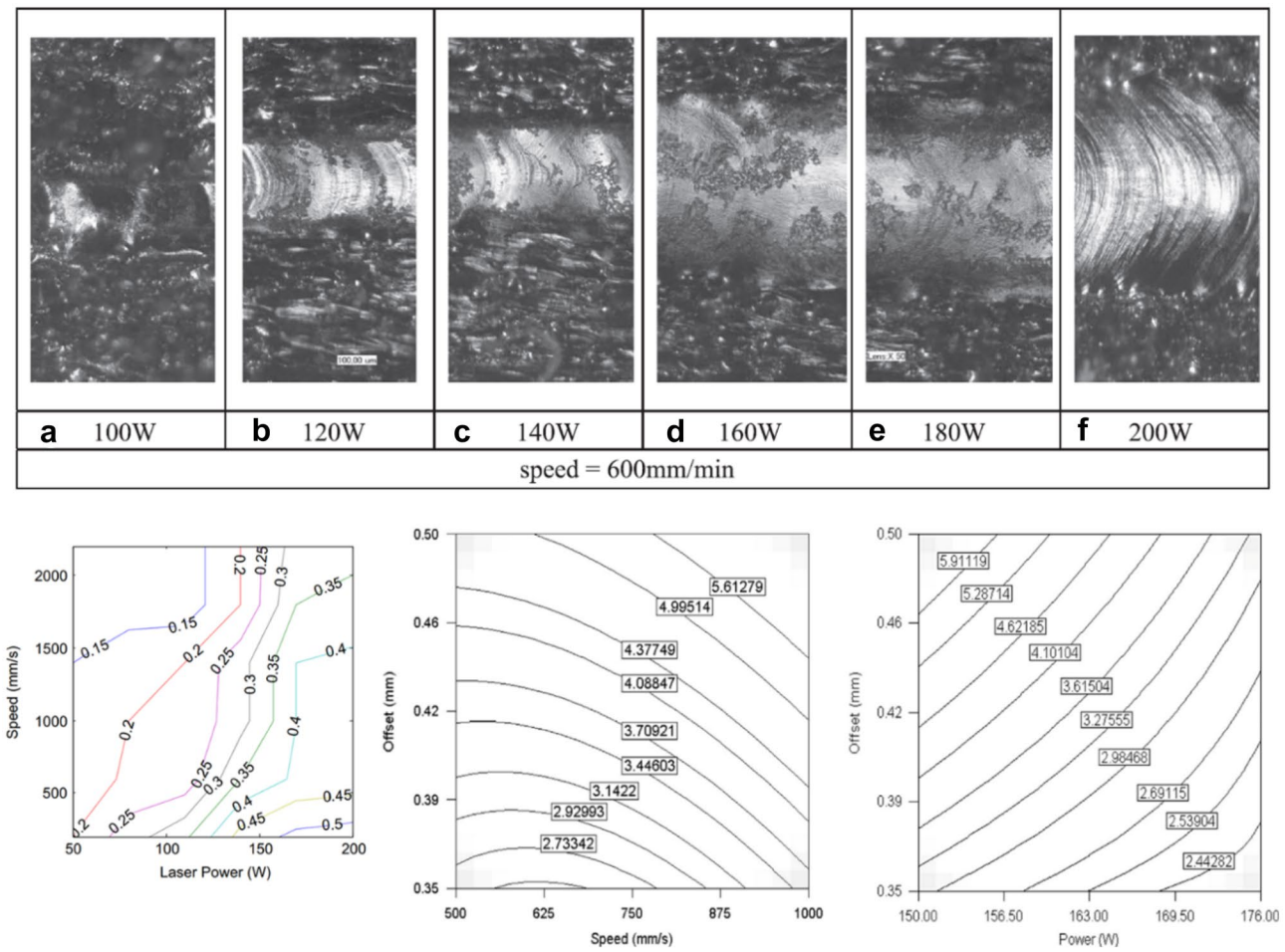

Fig. 26 Laser polishing of Ti-6Al-4 V selective laser melted components: (above) optical microscopic images of laser polished linear track for various laser power; (below) effect of power and speed on laser melted track width (number on line contour indicates melt width in mm) and interaction effect of power, speed and beam offset on surface roughness (numbers on the contour lines represent the surface roughness R_a in μm) [118]

depths exceeding 100 µm. With respect to the average surface roughness, however, this remelting depth is greater than necessary. Apart from major defects, below this depth, the remelting is of the order of the starting average surface roughness. In addition, the remelting is continuous but limited to a contour that follows the starting surface. The uniformity associated with the process suggests that if the surface defects in the starting SLM material are well identified, the remelting process can be calibrated to remove them [120].

Also Kahlin et al. [121] and Liang et al. [122] led fatigue testing after laser polishing process to examine improvements in fatigue strength of PBF Ti-6Al-4 V. Although in their investigations the roughness parameters were reduced by means of laser interaction, they did not observe significant increases in fatigue strength as compared to the parts in their as-built surface condition. In contrast, Lee et al. [123] have studied the effects of the laser polishing on the fatigue response of components made in Ti-6Al-4 V and manufactured by powder bed fusion. With laser polishing, in this case, the partially melted powder particles were successfully remelted onto the surface of the PBF Ti-6Al-4 V specimens, as the actual depth of laser polishing was greater than the maximum peak-valley depth, identified through the R_z parameter. By means of laser polishing, they then reconstructed the topography of the surface and, therefore, the sharpness of the surface profile which was found to be smoother. The high-cycle fatigue strength of laser polished specimens has been improved over specimens with as-built surfaces. The increase in high-cycle fatigue strength for laser polished specimens is related to the lower surface roughness (Fig. 27).

An interesting analytical approach, proposed by Alfieri et al. [124], aims to evaluate the post-processing treatment by laser on AM parts in stainless steel - grade 17–4 (UNS S17400) using a scanning head that allows to impose a beam oscillation on the laser beam. The guiding idea is imported from laser welding, where the oscillation of the laser beam along the scanning path is preferred over the conventional defocusing of the spot in order to preserve the required irradiation threshold and cover the space

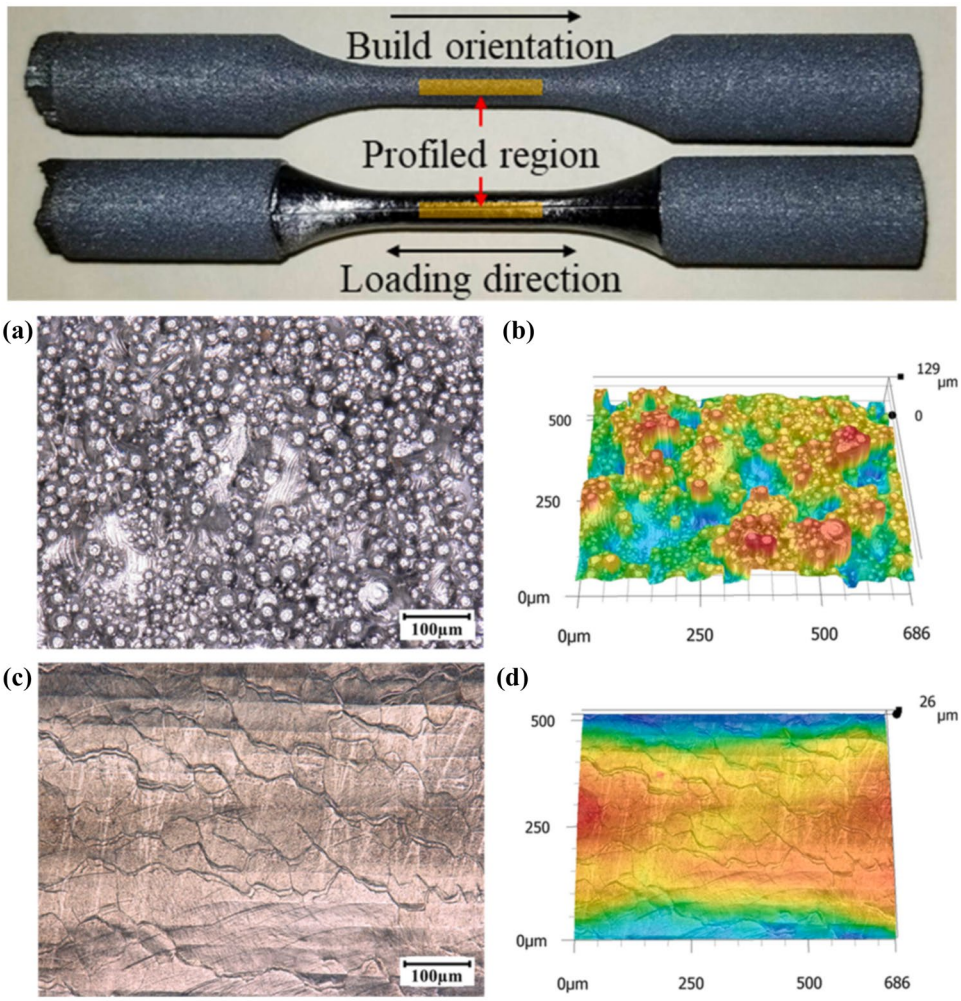

Fig. 27 Laser polishing on Ti-6Al-4 V parts manufactured using powder bed fusion [123]

between the adjacent irregular edges or the addition of the intermediate layer [125]. Shal et al. compared experimentally the conventional processes of laser welding and beam oscillation, observing that the oscillation of the laser beam improves the quality and integrity of the joint by expanding the bonding area and favoring the formation of a brittle lower melting zone in the region. Even Kuryntsev and Gilmutdinov [126] investigated a laser welding process using a constant laser beam trajectory and an oscillating trajectory. The results showed that after the second welding step, with oscillating trajectory of the laser beam, the central and top parts of the bead showed a lower microhardness than the root part. The oscillation passage of the laser beam ensured less shrinkage and greater ductility of the weld metal.

The analysis is faced in Alfieri et al. [124] on AM parts built according to three different orientations: flat built, 45° built, and up-right built, which therefore offer a different response in terms of stair case effect. It is possible to show that the surface topography can be improved and that the answer depends on the initial characteristics of the samples. In fact, important improvements are obtained on samples built at 45° and in a vertical position, as the process is able to reduce the arithmetic roughness below 2 μm on average. Less significant reductions were reached in the literature [127]. The oscillation of the laser beam offers specific advantages over linear scanning in that the effects of heat are less evident in both the melting zone and the HAZ, as shown by the Vickers microhardness tests and microscopic analysis. The oscillation offers the simultaneous advantages of a limited microstructural weakening of the material and a higher polishing speed. With an operating laser power of 1 kW and a processing speed of 2 m/min, oscillating with an amplitude of 2 mm at a frequency of 200 Hz is suggested. Moreover, the authors set the energy density on the order of 30 J/mm^2, basing on a value identified in literature as effective for the purpose of surface polishing [128, 129]. As for the laser path, an oscillating beam has been previously proposed in the literature [112], with a reduction of the roughness of up to 92% compared to parts produced with AlSi10Mg additives. However, in this case, a one-dimensional scanning system had been used.

The innovative laser polishing process based on the oscillation of the laser beam is applied by Caggiano et al. [130] on AM parts made of precipitation hardened Cr–Cu steel, widely used in the automotive industry. Different polishing conditions are examined, all based on the oscillation of the laser beam (Fig. 28), using a Yb:YAG source with a focused spot of 1 mm in diameter and an image field of 400 mm × 400 mm^2. The laser

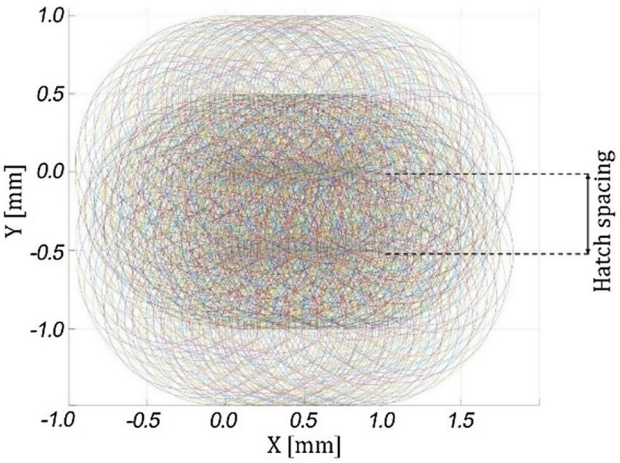

Fig. 28 Laser beam spot wobbling in multi-track scanning [130]

power P and the amplitude of oscillation were varied, respectively, in the range 400–600 W and 1.2 mm, while the processing speed and the oscillation frequency were kept constant at 1 m min and 200 Hz, respectively. The process of laser oscillation polishing in multitrack scan mode (with a ratio percentage of optimal overlap set at 50%) has provided a significant improvement in surface roughness between 62 and 78% according to the process conditions with respect to the surface of the as-built AM part, inducing rather limited microstructural changes. The depth of the melting zone is between 0.204 and 0.434 mm, and the extension of the HAZ is between 0.750 and 0.980 mm. The authors address the surface characterization also through the elaboration of machine learning–based images using neural convolutional networks (CNN), proving that they can be profitably used for the automation of the laser polishing process. A summary of main result of laser polishing treatment on SLM parts is, finally, reported in Table 1.

5 Analysis and applications of laser polishing: criticality and potentiality of the technology

Laser polishing can constitute a viable solution for the improvement of the surface finish of metal components. The application of the laser polishing and the results obtained at the end of the process depend mainly on the initial roughness of the surface and, therefore, also on the fabrication process of the specific component. Laser polishing is, therefore, an alternative to conventional surface finishing technologies based on chip removal. It can be

Table 1 Summary of the main results concerning laser polishing achieved in the literature

Material	Laser source	Polishing parameters	Roughness improvement	Other modifications	References
SLM on Inconel 718 superalloy	Nanosecond PW Fiber laser; spot diameter: 50 µm	Laser power of 90 W; scanning speed of 60–150 mm/s; overlap rate of laser spot 10%; inert gas Ar	R_a from 7.5 to 0.1 µm	Microhardness from 345 to 440 HV	[108]
SLM on AISI 316L steel	CW fiber laser Spot diameter 200 µm	Laser power of 50 W; scanning speed of 100 mm/s; 3 passes; overlap percentage 80%	R_a from 4.59 to 0.34 µm, reduction of 92.6%	Corrosion resistance	[110]
SLM on 18Ni (300 grade) Maraging steel	Nd:YAG Q-switch (using both CW and PW mode); Spot diameter: 100 µm	CW mode; laser power of 50 W; scanning speed of 300 mm/s and an hatch spacing of 25 µm	The upper surface has an initial R_a of 2.7 ± 0.6 µm, while the side surface presents an initial R_a of 6.4 ± 0.8 µm. After laser polishing, a R_a of less than 1 µm (minimum R_a 0.6 µm) is obtained regardless the initial roughness		[111]
SLM on AlSi10Mg alloy	Solid state disk laser; spot diameter of 430 µm; one dimensional scanner head	PW mode; laser power of 1700 W; laser frequency of 10 Hz; feeding rate of 40 mm/min; pulse overlap bigger than 50%; inert gas Ar	High reduction of the surface roughness from initially R_a = 8.7 µm to laser polished R_a = 0.66 µm. This represented a reduction of 92%		[112]
SLM on CoCr alloy	PW Fiber laser; Spot diameter: 50 µm; f-theta lens	On planar surface Laser Power of 70 W, Scanning speed 300 mm/s; Hatching space 0.03 mm; defocusing distance 6 mm	R_a from 4.23 to 0.73 µm reduction of over 90%	Surface hardness of the LP samples enhanced by 8%. Beneficial effect also on corrosion resistance (increase of 30%)	[113]
SLM on Inconel 718 superalloy	Laser system with a 1.8 kW HQ CO_2,	Laser power of 500 W; scan speed of 800–850 mm/min	Surface roughness below 2 µm, about 80% improved		[115]
LMD on AISI 316L steel	CW fiber laser source	Laser power 210 W; scan speed 3000 mm/min; overlap of the tracks 60%	Reduction of S_a from 21 to 0.79 µm		[116]
Digital Metal on AISI 316L steel	PW MOPA-based Yb-doped fiber nanosecond (ns) laser source; 3D scanning head	Average laser power of 37.2 W; pulse duration 220 ns; fluence 9 J/cm^2, single polishing pass; overlap factors 95% and 88–91% along beam scanning and step-over directions, respectively; both normal atmospheric and inert gas Ar conditions	Maximum reduction in surface Roughness of 94% (from ~3.8 to ~0.2 µm S_a)	Sub-surface microhardness improved of up to ~60% until a depth of ~90–100 µm; reduction in porosity; improved wear resistance	[117]

Table 1 (continued)

Material	Laser source	Polishing parameters	Roughness improvement	Other modifications	References
SLM on Ti6Al4V alloy	CW fiber laser source with a maximum power of 200 W and a laser spot of 500 µm	A track width of 0.41 mm and smooth surface morphology was achieved with a laser power range of 150–180 W and a speed range of 500–1000 mm/min. Laser powers below 150 W, or scanning speeds greater than 1000 mm/min, failed to produce a reasonable melt pool width. Powers higher than 180 W or scanning speeds less than 500 mm/min produced significant surface ripples. Inert gas Ar	Average surface roughness of the base material is around 10.2 µm. A minimum surface roughness of 2.4 µm R_a was achieved with a laser power of 160 W, scanning speed of 750 mm/min, and a beam offset of 0.35 mm		[118]
SLM on Inconel 625 alloy	200 W laser; spot size of 30 µm	Automated XYZ platform with 3-micron precision control integrated with a laser beam delivery system. The hardware insure that for each laser spot, during XYZ motion, only a specific predefined amount of laser energy is deposited. Average power 5–10 W; average XY velocity 4 mm/s; 2 psig argon	Improvement of surface roughness. The polishing trials led to the formation of an oxide film. Remelting layer depth was 100–200 µm	Laser remelting does not appear to improve fatigue life	[119, 120]
PBF on Ti6Al4V alloy	CW fiber laser coupled to a galvo scanner with an f-theta lens; spot size of approximately 15 µm	Laser power of 120 W, scanning speed of 100 mm/s and hatching space of 10 µm; argon inert gas	The LP successfully decreased all roughness parameters by 60–70%. Among the investigated roughness parameters the maximum valley depth of the profiled line (R_v) showed the biggest reduction (~69%). Reduction of R_a from 14.23 ± 3.28 µm to 6.01 ± 1.63 µm; reduction of R_z from 90.58 ± 19.72 µm to 28.02 ± 5.43 µm	High-cycle fatigue lives of the laser polished parts were somewhat longer than the as-built specimens due to reduced surface roughness	[123]
SLM on stainless steel — grade 17–4 (UNS S17400)	EOSINT M270 commercial laser sintering system (EOS, Krailling, Germany)	Laser power 1 kW; scanning speed 2 m/min; oscillating with an amplitude of 2 mm at a frequency of 200 Hz; energy density on the order of 30 J/mm^2	From an initial R_a of about 15 µm, a reduction of R_a below 2 µm is obtainable, on average	Change in the microstructure is induced, and specific benefits are offered by laser beam wobbling (LBW) compared with linear scanning (LS). Heat effect is proven to be lower. Microhardness is of about 275 $HV_{0.2}$ for LBW compared to 265$HV_{0.2}$ for LS	[124]

Table 1 (continued)

Material	Laser source	Polishing parameters	Roughness improvement	Other modifications	References
SLM on Cr-Cu steel	Yb:YAG Laser source; focused spot diameter of 1 mm in; f-theta lens	Laser power in the range 400–600 W; amplitude oscillation of 1.2 mm; scanning speed 1 m/min; oscillation frequency constant at 200 Hz; percentage of overlap set at 50%	Significant improvement in surface roughness between 62 and 78%	Laser polishing inducing rather limited microstructural changes. Depth of the melting zone is between 0.204 and 0.434; HAZ is between 0.750 and 0.980 mm	[130]

applied to any metal material as shown in Fig. 29, using different types of laser sources in continuous or pulsed mode, defocusing the beam in most practical cases, working on linear and non-linear scans, or by oscillating the beam.

Nowadays, laser polishing is broadly used on real components (not only on part of them). In recent time, it is spreading to a greater extent in the industrial and biomedical sectors. In the industrial field, the process is used with both continuous and pulsed sources. In the fabrication of tools and molds, laser polishing technologies can be, generally, used as a device for the improvement of selected areas that are subject to greater wear (Fig. 30). The results achievable are remarkable, since it is possible to obtain improvements in the average roughness of up to 80% with processing times of the order of tens of seconds per square centimeter and, very often, an increase in the surface hardness in the remelted layer.

In the field of biomedical engineering, the laser is used for post-processing of biomedical devices and surgical instruments to decrease defects, surface ridges, and even sharp edges that would favor contamination with bacteria. The most used material in the biomedical field is titanium, which, even if it is very hard-to-cut, features high biocompatibility.

Examples of applications in the medical field are shown in Fig. 31a, where the first component is for a dental implant. Instead, Fig. 31b shows the polishing work for a ventricular assist device (VAD). Beyond to being manufactured with a difficult-to-process material like titanium, both components are characterized by a very complex geometry. Adoption of laser polishing for workpiece with complex geometry can lead to a reduction both in costs and of up to 30% in the manufacturing time of the component, as well as to a significant reduction of the environmental impact [64]. This is because the polishing of components with complex geometry (for example, the abovementioned items for dental implants or molds for the massive production of components both in metal and plastic materials) is still handmade by qualified personnel. Similarly, in industrial optics, where difficult-to-cut materials are combined with complex geometry, laser polishing is confirmed as a winning and competitive technology, especially when fully automated (Fig. 32).

Laser polishing can, therefore, boast significant advantages in the surface finishing of difficult-to-machine and complex-shaped items. As seen, titanium components, obtained using conventional technologies, are defined as “hard to cut” and do not suite well to technologies based on chip removal. So, the adoption of laser processing can represent a beneficial alternative [132, 133]. For components produced by additive manufacturing, on the other hand, given the very common high complexity of

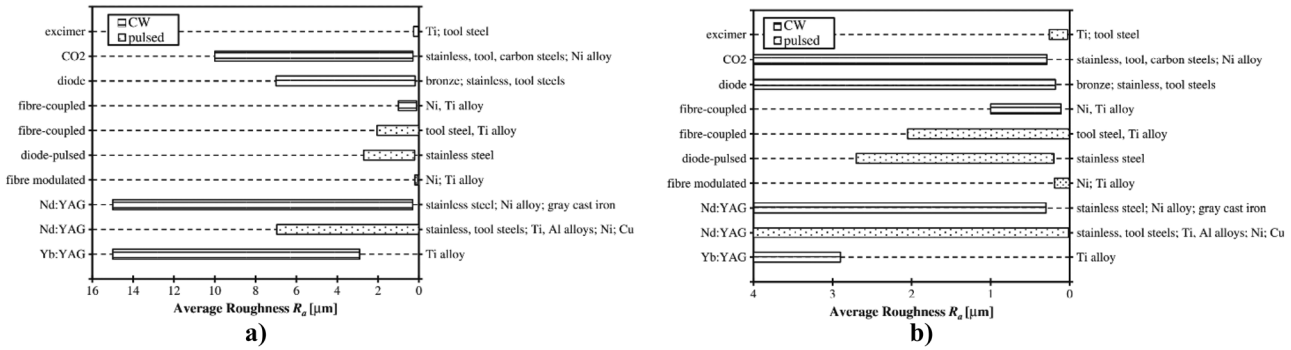

Fig. 29 Correlation between sources, materials, and surface quality [131]

the workpiece, the material is not a discriminating factor anymore. In fact, regardless of the material, laser polishing is a viable process for processing alloys that would be impossible to finish differently. In addition, most additive manufacturing technologies for metal components are based on lasers. Hence, the device used to manufacture the component can be equipped with a laser source and a scanning system to be devoted to laser polishing, as well. In some cases, to adopt laser polishing technology, it is not necessary to invest in the purchase of a second source, since the device already has it inside, with significant savings for the manufacturers. In SLM, for example, once the first stage of manufacturing process is finished, the component is ready,the excess powders can be removed and then recycled. The second stage would consist in the polishing process, which could take place in the same chamber in an inert environment. The same equipment could be, thus, used, at the same time, for both the manufacturing of the complex-shaped workpiece and, after that, for its polishing.

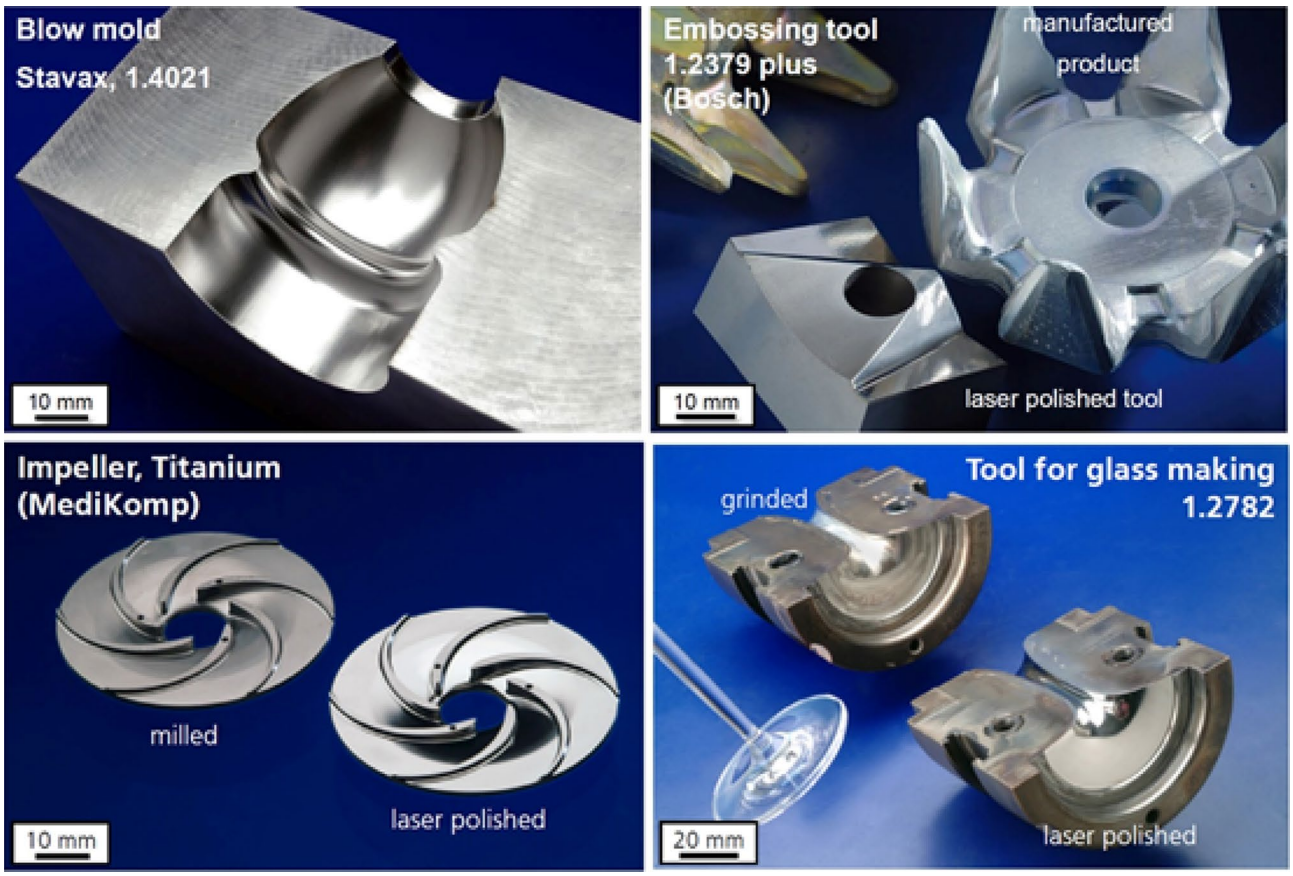

Fig. 30 Laser polishing applications (source: Fraunhofer ILT, Laser material Processing, Polishing, Aachen, Germany)

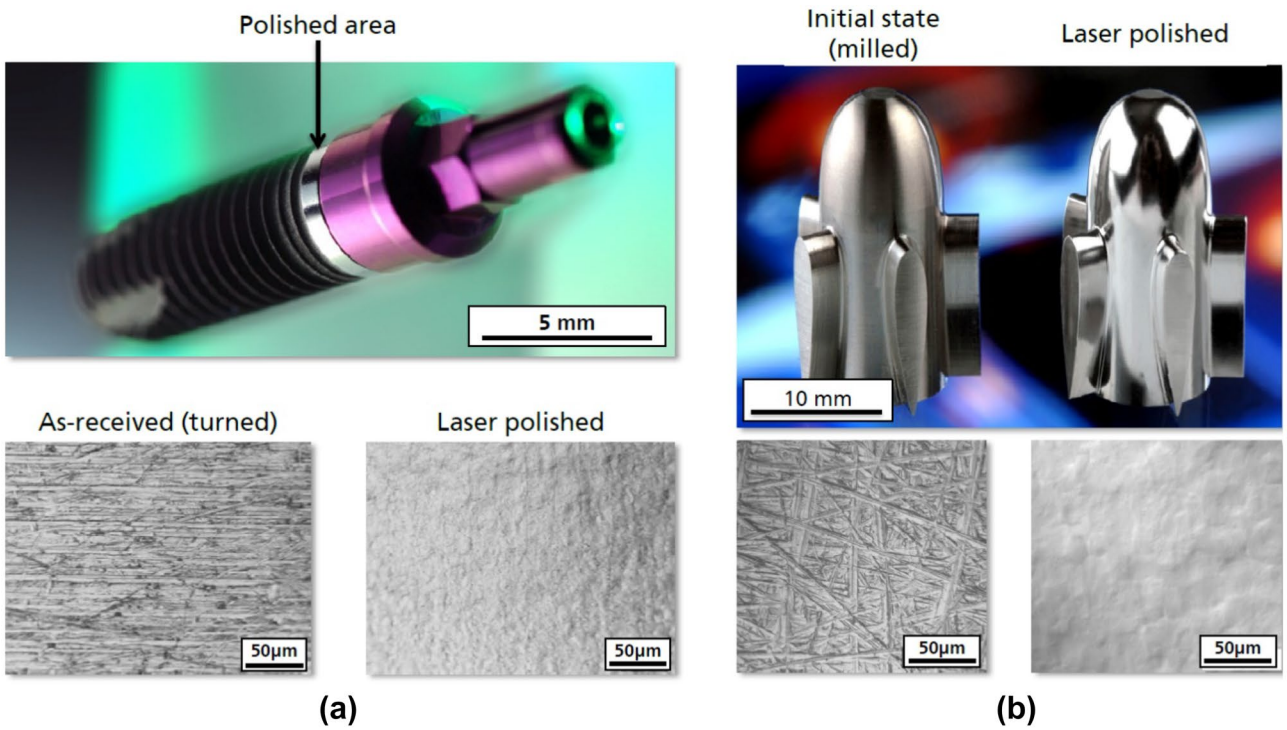

Fig. 31 Examples in the medical field: (**a**) dental implant (**b**) ventricular assist device (VAD) (source: Fraunhofer ILT, Laser material processing, Polishing, Aachen, Germany)

However, due to the development of new manufacturing techniques that allow to fabricate components with increasingly complex geometry in many industrial segments, there is no solution today that can be universally applied for the improvement of surface finishing of all of them. Thanks to the aid of CAM software and CNC multi-axis systems, it is, however, possible, starting from digital data, to create toolpath with different strategies for laser polishing [134]. This is a very effective and low cost automation strategy that is particularly convenient and easy to develop in the case of components produced by additive manufacturing. In fact, the digital data, which represents the discretization of the virtual model, allows to start the manufacturing process (AM), and generates the components, can be also used

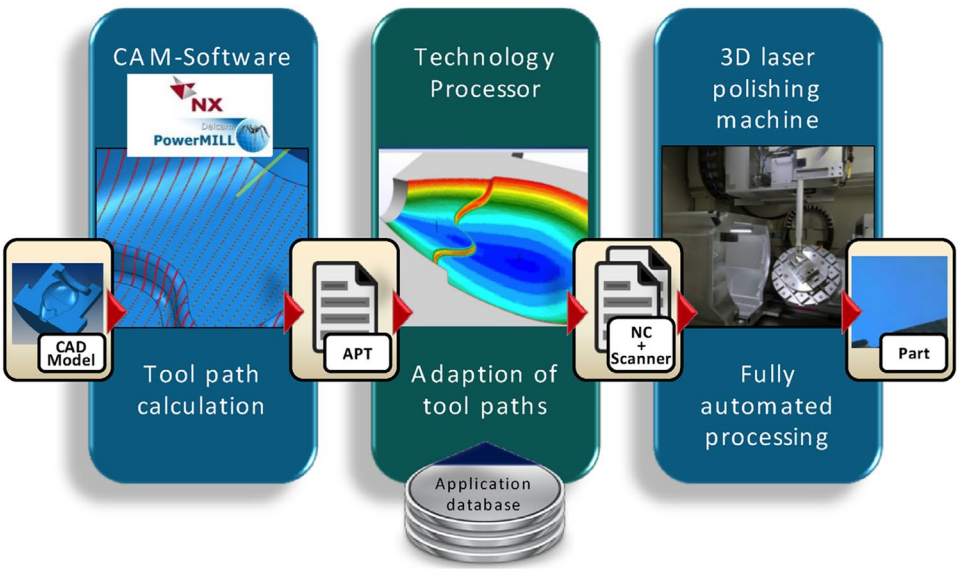

Fig. 32 CAM-NC process chain for laser polishing [134]

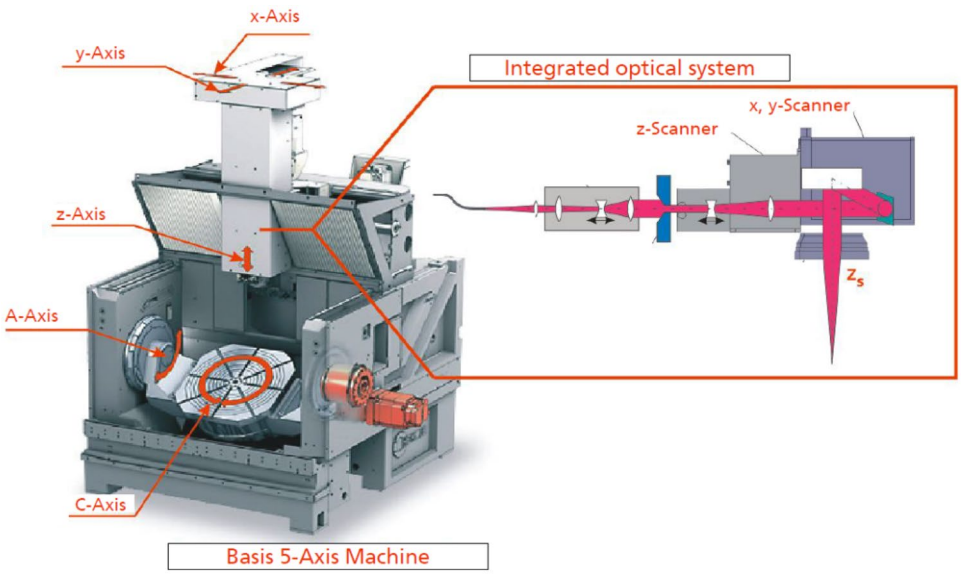

Fig. 33 Schematics of the laser polishing machine: 5-axis machine movement system (Hermle) with the integrated 3D optical scanning system [135]

for their post-processing. Specifically, those digital data can be used for the development of laser polishing toolpaths, simplifying, by far, the routine to post-process each specific component.

Laser polishing of complex-shaped and hard-to-cut components is also made much more effective thanks to the development of scanning devices in which the laser beam is moved by galvanometric systems and then focused through f-theta lenses. This particular type of focusing lens allows to have considerable benefits as the scanning head can remain stationary. Accordingly, the laser beam that remains focused on the plane can move at almost constant speeds. This can limit the drawbacks deriving from accelerations, thus supplying the material with the same amount of power during post-processing.

Processing time in industries is crucial and laser polishing makes no exception. Therefore, an additional issue that must be taken into account concerns the possibility of increasing the process speed for large workpiece, regardless the shape and type of material being involved. First, higher laser powers can be set by defocusing the beam in order to obtain the same surface energy density, while processing a much larger portion of the surface in an equivalent time frame. Very large laser spots also allow to set high h_s, so that, once the scanning strategy is set, the process time drops significantly. A second solution is to use robotic arms that can cover much larger distances than those achievable in a 5-axis CNC system. In this respect, more sophisticated CNC systems are being developed. They will allow to manage 5 + 3 axes, simplifying the simultaneous positioning and polishing of the workpiece (Fig. 33). These systems will increase the number of strategies that could be applied to post-process 3D components fabricated by AM technologies [135], increasing the overall effectiveness of the process.

Laser polishing can also be profitably used to ease the manufacture of full density or near full density components [136–138]. The powder bed is made up of numerous voids. Since the process is repeated for each layer, it is difficult to obtain components with 100% density, even if, by optimizing the process parameters, it is possible to get very close to that value. Once the layer n is complete, the surface can be "remelted" during fabrication, just like in the laser polishing process. The difference is that the "polished" surface will subsequently be covered by the layer $n+1$, and, therefore, it will not be visible anymore. This mechanism allows to increase the density of the component by reducing its internal porosities. In any case, since laser polishing is a thermal process, the energy transported by the laser beam could thermally alter the machined surface and particular attention must be paid to the cooling methods of the component. For example, if the cooling is too rapid, in the machining of martensitic steels, a martensitic layer could be formed, which would considerably increase the hardness in the thermally altered zone. For stainless steels, on the other hand, slow cooling is harmful as it would lead to the precipitation of chromium carbides ($Cr_{23}C_6$) in the areas with a high energy content (grain boundaries). In this way, the area immediately adjacent to the edge is depleted in Cr, reducing the corrosion resistance of the material itself. Thus, the chromium-poor zone would act as an anode while the grain boundary and the grain core, rich in Cr (noble element), would act as the cathode. A harmful corrosion phenomenon known as "knife corrosion," localized and not visible on the surface, could be favored. However, the energy is supplied quickly by the laser beam and, therefore, cooling always takes place at sufficiently high solidification speeds, avoiding the problems described above.

Similarly, all the issues relating to heat treatments during laser polishing must also be taken into consideration.

Many metal components need to be heat treated at the end of the manufacturing process, so partial heat alteration during polishing may not be a problem. However, this applies differently to SLM and EBM. The heat source is different in the two processes. In SLM, lasers with maximum powers of 400 W are used, while in EBM, an electron beam is used. The temperature reached on the powder bed for EBM technology is typically higher and this is the reason why the metal powders used in EBM are larger than those used in SLM. If the temperature variation is considered compared to that of the chamber, the EBM technology will have the highest temperature "delta." In this regard, in EBM, a preheating of the powder bed is always provided during the process and, for this reason, it is defined as a "hot" process. In SLM, on the other hand, the temperatures reached are much lower and it is therefore not necessary to pre-heat the powder bed (i.e., "cold" process). Consequently, the cooling of the components during the process will be much faster in SLM than in EBM, where it is necessary, at the end of the process, to let the component cool before removing it from the machine. Therefore, in SLM, unlike the foundry, the fabrication of components with complex geometry and thin wall, because of the rapid cooling, is preferred. While in EBM, the manufacturing of massive components is preferred as the cooling is slower. Looking at the residual stresses, these will certainly be present in the components produced in SLM (rapid solidification), while due to the slow cooling, they will be less strong in EBM (slower solidification). Therefore, a stress relieving heat treatment at the end of the process is necessary for the components produced in SLM, while it is not so for those produced in EBM. Indeed, the possible thermal alteration and structural modifications of the components caused by laser polishing would not constitute a major problem in SLM. In fact, the component, in any case, will have to undergo a subsequent stress relieving heat treatment after SLM. Accordingly, subsequent treatments can be designed, even in the same oven, to obtain the desired structure. In EBM, on the other hand, in general, no heat treatments are envisaged since the component has no residual stresses. Therefore, possible thermal alterations induced of the EBM components by laser polishing could be an issue. Also, from a cost point of view, in SLM systems, an oven for heat treatments is always available, while it is not to be expected if EBM technology is used. In any case, it must also be emphasized that the EBM technology, due to the use of larger metal powders, achieves worse surface roughness. The choice of the post-processing process, therefore, should always be made by looking at the surface quality specifications required by the designer and evaluating, in terms of time and cost, which, of the many available technologies for complex geometry components, is the most advantageous.

6 Conclusions

The applications of laser polishing technology are multifold. In recent years, this technology is increasingly used for components fabricated by additive manufacturing. Additive manufacturing is constantly evolving, and, nowadays, it is no longer considered solely as a tool for rapid prototyping, but it is increasingly becoming a manufacturing technology. Consequently, if laser polishing is one of the solutions for the advantageous "post-processing" for some AM technologies, it can be also widely used in many industrial fields, including the production of aircraft engines, combustion chambers for aerospace launchers, systems for neurosurgery, and structural components for vehicles. These are all industrial sectors in which additive manufacturing is increasingly being used as winning technology. In addition to the fields mentioned above, laser polishing technology can also assert itself in all those sectors where it is necessary to find new solutions to highly complex scientific and technical problems, especially when dealing with complex-shaped and hard-to-cut workpiece.

In conclusion, the future challenges of laser polishing technology will concern the following: (i) the reduction of the high investment costs initially necessary to access the technology, especially due to the high automation required and the need to operate in inert atmospheres; (ii) the presence of the diffraction limit of the laser beam which limits the maximum resolution of the processing; (iii) the objective difficulties in managing large surfaces with long operating distances (> 1 mm); (iv) the removal of any processing residues that may alter the surfaces; (v) the increase in process speeds without reducing the ability to control the operating parameters; (vi) the effectiveness on surfaces previously finished with mechanical technologies. Overcoming these limits could greatly extend the field of use of laser polishing technologies, with significant benefits in terms of cost reduction, processing times, and environmental footprint.

Author contribution The contribution of the authors to the study conception, design, material preparation, data collection, and analysis is equal. The first draft of the manuscript was written by Prof. Annamaria Gisario. Prof. Massimiliano Barletta revised the manuscript. All authors read and approved the final manuscript.

Data availability Data will be made available on reasonable request.

Code availability Not applicable.

Declarations

Consent to participate Not applicable.

Consent for publication Not applicable.

Conflict of interest The authors declare no competing interests. No ethical approval is required.

References

1. DebRoy T, Wei HLL, Zuback JSS, Mukherjee T, Elmer JWW, Milewski JOO, Beese AMM (2018) 286 A. Wilson-Heid, A. De. W Zhang Prog Mater Sci 92:112–224
2. Frazier WE (2014) Metal additive manufacturing: a review. J Mater Eng Perform 23:1917–1928. https://doi.org/10.1007/s11665-014-0958-z
3. Gibson I, Rosen D, Stucker B (2010) Additive manufacturing technologies – rapid prototyping to direct digital manufacturing. Additive manufacturing technologies: rapid prototyping to direct digital manufacturing. https://doi.org/10.1007/978-1-4419-1120-9
4. Herzog D, Seyda V, Wycisk E, Emmelmann C (2016) Additive manufacturing of metals. Acta Mater 117:371–392. https://doi.org/10.1016/j.actamat.2016.07.019
5. Kannan GB, Rajendran DK (2017) A review on status of research in metal additive manufacturing. In: Wimpenny DI, Pandey PM, Kumar LJ (Eds.) Advances in 3D printing & additive manufacturing technologies. Springer, Singapore, pp. 95–100. https://doi.org/10.1007/978-981-10-0812-2_8
6. Milewski JO (2017) Understanding metal for additive manufacturing. In: Milewski JO (Ed.) Additive manufacturing of metals: from fundamental technology to rocket nozzles, medical implants, and custom jewelry. Springer Series in Materials Science. Springer International Publishing, Cham, pp. 49–83. https://doi.org/10.1007/978-3-319-58205-4_4
7. Srivastava M, Rathee S, Maheshwari S, Kundra TK (2019) Additive manufacturing: fundamentals and advancements. CRC Press
8. Wong KV, Hernandez A (2012) A review of additive manufacturing. ISRN Mechanical Engineering 2012:1–10. https://doi.org/10.5402/2012/208760
9. Hull CW (1984) Apparatus for production of three-dimensional objects by stereolithography. United States Patent, Appl., No. 638905, Filed
10. Tofail SAM, Koumoulos EP, Bandyopadhyay A, Bose S, O'Donoghue L, Charitidis C (2018) Additive manufacturing: scientific and technological challenges, market uptake and opportunities. Mater Today 21:22–37. https://doi.org/10.1016/j.mattod.2017.07.001
11. F42 Committee (2015) Terminology for additive manufacturing technologies. ASTM International. https://doi.org/10.1520/F2792-12A
12. Chlebus E, Kuźnicka B, Kurzynowski T, Dybała B (2011) Microstructure and mechanical behaviour of Ti-6Al-7Nb alloy produced by selective laser melting. Mater Charact 62:488–495. https://doi.org/10.1016/j.matchar.2011.03.006
13. Edwards P, O'conner A, Ramulu M (2013) Electron beam additive manufacturing of titanium components: properties and performance. J Manuf Sci Eng 135. https://doi.org/10.1115/1.4025773
14. Gokuldoss PK, Kolla S, Eckert J (2017) Additive manufacturing processes: selective laser melting, electron beam melting and binder jetting—selection guidelines. Materials 10:672. https://doi.org/10.3390/ma10060672
15. Gong X, Anderson T, Chou K (2013) Review on powder-based electron beam additive manufacturing technology. Presented at the ASME/ISCIE 2012 International Symposium on Flexible Automation. American Society of Mechanical Engineers Digital Collection, pp. 507–515. https://doi.org/10.1115/ISFA2012-7256
16. Kim J, Lee WJ, Park HW (2016) The state of the art in the electron beam manufacturing processes. Int J Precis Eng Manuf 17:1575–1585. https://doi.org/10.1007/s12541-016-0184-8
17. Körner C (2016) Additive manufacturing of metallic components by selective electron beam melting — a review. Int Mater Rev 61:361–377. https://doi.org/10.1080/09506608.2016.1176289
18. Murr LE, Gaytan SM, Ramirez DA, Martinez E, Hernandez J, Amato KN, Shindo PW, Medina FR, Wicker RB (2012) Metal fabrication by additive manufacturing using laser and electron beam melting technologies. J Mater Sci Technol 28:1–14. https://doi.org/10.1016/S1005-0302(12)60016-4
19. Zhao X, Li S, Zhang M, Liu Y, Sercombe TB, Wang S, Hao Y, Yang R, Murr LE (2016) Comparison of the microstructures and mechanical properties of Ti–6Al–4V fabricated by selective laser melting and electron beam melting. Mater Des 95:21–31. https://doi.org/10.1016/j.matdes.2015.12.135
20. Markusson L (2017) Powder characterization for additive manufacturing processes
21. Zhou J, Liao C, Shen H, Ding X (2019) Surface and property characterization of laser polished Ti6Al4V. Surf Coat Technol 380:125016. https://doi.org/10.1016/j.surfcoat.2019.125016
22. Charles A, Elkaseer A, Thijs L, Hagenmeyer V, Scholz S (2019) Effect of process parameters on the generated surface roughness of down-facing surfaces in selective laser melting. Appl Sci 9:1256. https://doi.org/10.3390/app9061256
23. Kamarudin K, Wahab MS, Shayfull Z, Ahmed A, Raus AA (2016) Dimensional accuracy and surface roughness analysis for AlSi10Mg produced by selective laser melting (SLM). MATEC Web Conf 78:01077. https://doi.org/10.1051/matecconf/20167801077
24. Childerhouse T, Jackson M (2019) Near net shape manufacture of titanium alloy components from powder and wire: a review of state-of-the-art process routes. Metals 9:689. https://doi.org/10.3390/met9060689
25. Mumtaz K, Hopkinson N (2009) Top surface and side roughness of Inconel 625 parts processed using selective laser melting. Rapid Prototyping Journal 15:96–103. https://doi.org/10.1108/13552540910943397
26. Calignano F (2018) Investigation of the accuracy and roughness in the laser powder bed fusion process. Virtual and Physical Prototyping 13:97–104. https://doi.org/10.1080/17452759.2018.1426368
27. Delfs P, Tows M, Schmid H-J (2016) Optimized build orientation of additive manufactured parts for improved surface quality and build time. Additive Manufacturing, Special Issue on Modeling & Simulation for Additive Manufacturing 12:314–320. https://doi.org/10.1016/j.addma.2016.06.003
28. Leon A, Aghion E (2017) Effect of surface roughness on corrosion fatigue performance of AlSi10Mg alloy produced by Selective Laser Melting (SLM). Mater Charact 131:188–194. https://doi.org/10.1016/j.matchar.2017.06.029
29. Majeed A, Lv J, Zhang Y, Muzamil M, Waqas A, Shamim K, Qureshi ME, Zafar F (2019) An investigation into the influence of processing parameters on the surface quality of AlSi10Mg parts by SLM process. In: 2019 16th International Bhurban Conference on Applied Sciences and Technology (IBCAST).

Presented at the 2019 16th International Bhurban Conference on Applied Sciences and Technology (IBCAST), pp. 143–147. https://doi.org/10.1109/IBCAST.2019.8667175
30. Nguyen QB, Luu DN, Nai SML, Zhu Z, Chen Z, Wei J (2018) The role of powder layer thickness on the quality of SLM printed parts. Archiv Civ Mech Eng 18:948–955. https://doi.org/10.1016/j.acme.2018.01.015
31. Tian Y, Tomus D, Rometsch P, Wu X (2017) Influences of processing parameters on surface roughness of Hastelloy X produced by selective laser melting. Addit Manuf 13:103–112. https://doi.org/10.1016/j.addma.2016.10.010
32. Vayssette B, Saintier N, Brugger C, El May M (2020) Surface roughness effect of SLM and EBM Ti-6Al-4V on multiaxial high cycle fatigue. Theoret Appl Fract Mech 108:102581. https://doi.org/10.1016/j.tafmec.2020.102581
33. Wang D, Liu Y, Yang Y, Xiao D (2016) Theoretical and experimental study on surface roughness of 316L stainless steel metal parts obtained through selective laser melting. Rapid Prototyping Journal 22:706–716. https://doi.org/10.1108/RPJ-06-2015-0078
34. Fousová M, Vojtěch D, Doubrava K, Daniel M, Lin C-F (2018) Influence of inherent surface and internal defects on mechanical properties of additively manufactured Ti6Al4V alloy: comparison between selective laser melting and electron beam melting. Materials 11:537. https://doi.org/10.3390/ma11040537
35. Rafi HK, Karthik NV, Gong H, Starr TL, Stucker BE (2013) Microstructures and mechanical properties of Ti6Al4V parts fabricated by selective laser melting and electron beam melting. J of Materi Eng and Perform 22:3872–3883. https://doi.org/10.1007/s11665-013-0658-0
36. Triantaphyllou A, Giusca CL, Macaulay GD, Roerig F, Hoebel M, Leach RK, Tomita B, Milne KA (2015) Surface texture measurement for additive manufacturing. Surf Topogr: Metrol Prop 3:024002. https://doi.org/10.1088/2051-672X/3/2/024002
37. Weißmann V, Drescher P, Bader R, Seitz H, Hansmann H, Laufer N (2017) Comparison of single Ti6Al4V struts made using selective laser melting and electron beam melting subject to part orientation. Metals 7:91. https://doi.org/10.3390/met7030091
38. Strano G, Hao L, Everson RM, Evans KE (2013) Surface roughness analysis, modelling and prediction in selective laser melting. J Mater Process Technol 213:589–597. https://doi.org/10.1016/j.jmatprotec.2012.11.011
39. Whitehouse DJ (2000) Surface characterization and roughness measurement in engineering. In: Rastogi PK (Ed.), Photomechanics, topics in applied physics. Springer, Berlin, Heidelberg, pp. 413–461. https://doi.org/10.1007/3-540-48800-6_12
40. Bača A, Konečná R, Nicoletto G, Kunz L (2015) Effect of surface roughness on the fatigue life of laser additive manufactured Ti6Al4V alloy. Manuf Technol 15:498–502. https://doi.org/10.21062/ujep/x.2015/a/1213-2489/MT/15/4/498
41. Gockel J, Sheridan L, Koerper B, Whip B (2019) The influence of additive manufacturing processing parameters on surface roughness and fatigue life. Int J Fatigue 124:380–388. https://doi.org/10.1016/j.ijfatigue.2019.03.025
42. Greitemeier D, Dalle Donne C, Syassen F, Eufinger J, Melz T (2016) Effect of surface roughness on fatigue performance of additive manufactured Ti–6Al–4V. Mater Sci Technol 32:629–634. https://doi.org/10.1179/1743284715Y.0000000053
43. Yadollahi A, Mahtabi MJ, Khalili A, Doude HR, Newman JC (2018) Fatigue life prediction of additively manufactured material: effects of surface roughness, defect size, and shape. Fatigue Fract Eng Mater Struct 41:1602–1614. https://doi.org/10.1111/ffe.12799
44. Hilbert LR, Bagge-Ravn D, Kold J, Gram L (2003) Influence of surface roughness of stainless steel on microbial adhesion and corrosion resistance. Int Biodeterior Biodegradation 52:175–185. https://doi.org/10.1016/S0964-8305(03)00104-5
45. Timoshevskii V, Ke Y, Guo H, Gall D (2008) The influence of surface roughness on electrical conductance of thin Cu films: an ab initio study. J Appl Phys 103:113705. https://doi.org/10.1063/1.2937188
46. Gadelmawla ES, Koura MM, Maksoud TMA, Elewa IM, Soliman HH (2002) Roughness parameters. J Mater Process Technol 123:133–145. https://doi.org/10.1016/S0924-0136(02)00060-2
47. Asiltürk İ, Çunkaş M (2011) Modeling and prediction of surface roughness in turning operations using artificial neural network and multiple regression method. Expert Syst Appl 38:5826–5832. https://doi.org/10.1016/j.eswa.2010.11.041
48. Benardos PG, Vosniakos G-C (2003) Predicting surface roughness in machining: a review. Int J Mach Tools Manuf 43:833–844. https://doi.org/10.1016/S0890-6955(03)00059-2
49. Choudhury IA, El-Baradie MA (1997) Surface roughness prediction in the turning of high-strength steel by factorial design of experiments. Proceedings of the International Conference on Mechanics of Solids and Materials Engineering. J Mater Process Technol 67:55–61. https://doi.org/10.1016/S0924-0136(96)02818-X
50. Çolak O, Kurbanoğlu C, Kayacan MC (2007) Milling surface roughness prediction using evolutionary programming methods. Mater Des 28:657–666. https://doi.org/10.1016/j.matdes.2005.07.004
51. Hasegawa M, Seireg A, Lindberg RA (1976) Surface roughness model for turning. Tribol Int 9:285–289. https://doi.org/10.1016/0301-679X(76)90019-0
52. Muñoz-Escalona P, Maropoulos PG (2015) A geometrical model for surface roughness prediction when face milling Al 7075–T7351 with square insert tools. J Manuf Syst 36:216–223. https://doi.org/10.1016/j.jmsy.2014.06.011
53. Puertas Arbizu I, Luis Pérez CJ (2003) Surface roughness prediction by factorial design of experiments in turning processes. Proceedings of the International Conference on the Advanced Materials Processing Technology. J Mater Process Technol 2001(143–144):390–396. https://doi.org/10.1016/S0924-0136(03)00407-2
54. Saï K, Bouzid W (2005) Roughness modeling in up-face milling. Int J Adv Manuf Technol 26:324–329. https://doi.org/10.1007/s00170-004-2305-2
55. Ahn D, Kim H, Lee S (2009) Surface roughness prediction using measured data and interpolation in layered manufacturing. J Mater Process Technol 209:664–671. https://doi.org/10.1016/j.jmatprotec.2008.02.050
56. Wu D, Wei Y, Terpenny J (2018) Surface roughness prediction in additive manufacturing using machine learning. Presented at the ASME 2018 13th International Manufacturing Science and Engineering Conference. American Society of Mechanical Engineers Digital Collection. https://doi.org/10.1115/MSEC2018-6501
57. Seabra M, Azevedo J, Araújo A, Reis L, Pinto E, Alves N, Santos R, Pedro Mortágua J (2016) Selective laser melting (SLM) and topology optimization for lighter aerospace componentes. Procedia Structural Integrity, XV Portugese Conference on Fracture, PCF 2016, 10–12 February 2016. Paco de Arcos, Portugal 1:289–296. https://doi.org/10.1016/j.prostr.2016.02.039
58. Wang Y, Xia J, Luo Z, Yan H, Sun J, Lü E (2020) Self-supporting topology optimization method for selective laser melting. Addit Manuf 36:101506. https://doi.org/10.1016/j.addma.2020.101506
59. Strano G, Hao L, Everson R, Evans K (2013). A new approach to the design and optimisation of support structures in additive manufacturing. https://doi.org/10.1007/S00170-012-4403-X
60. Bartolo PJ (2011) Innovative developments in virtual and physical prototyping. Proceedings of the 5th International Conference on Advanced Research in Virtual and Rapid Prototyping, Leiria, Portugal, 28 September - 1 October, 2011. CRC Press
61. Maconachie T, Leary M, Lozanovski B, Zhang X, Qian M, Faruque O, Brandt M (2019) SLM lattice structures:

properties, performance, applications and challenges. Mater Des 183:108137. https://doi.org/10.1016/j.matdes.2019.108137
62. Nazir A, Abate KM, Kumar A, Jeng J-Y (2019) A state-of-the-art review on types, design, optimization, and additive manufacturing of cellular structures. Int J Adv Manuf Technol 104:3489–3510. https://doi.org/10.1007/s00170-019-04085-3
63. Gillespie LK (2006) Mass finishing handbook, 1st, edition. Industrial Press Inc, New York
64. Krishnan A, Fang F (2019) Review on mechanism and process of surface polishing using lasers. Front Mech Eng 14:299–319. https://doi.org/10.1007/s11465-019-0535-0
65. Perry TL, Werschmoeller D, Li X, Pfefferkorn FE, Duffie NA (2009) Micromelting for laser micro polishing of meso/micro metallic components. Presented at the ASME 2007 International Manufacturing Science and Engineering Conference, American Society of Mechanical Engineers Digital Collection, pp. 363–369. https://doi.org/10.1115/MSEC2007-31173
66. Nüsser C, Sändker H, Willenborg E (2013) Pulsed laser micro polishing of metals using dual-beam technology. Physics Procedia, Lasers in Manufacturing (LiM 2013) 41:346–355. https://doi.org/10.1016/j.phpro.2013.03.087
67. Nüsser C, Wehrmann I, Willenborg E (2011) Influence of intensity distribution and pulse duration on laser micro polishing. Physics Procedia, Lasers in Manufacturing 2011- Proceedings of the Sixth International WLT Conference on Lasers in Manufacturing 12:462–471. https://doi.org/10.1016/j.phpro.2011.03.057
68. Temmler A, Liu D, Luo J, Poprawe R (2020) Influence of pulse duration and pulse frequency on micro-roughness for laser micro polishing (LμP) of stainless steel AISI 410. Appl Surf Sci 510:145272. https://doi.org/10.1016/j.apsusc.2020.145272
69. Hua M, SeDao, Shao TM, Tam HY (2007) Surface transformation of DF-2 steel after continuous mode laser irradiation. Journal of Materials Processing Technology, 192-193:89–96. https://doi.org/10.1016/j.jmatprotec.2007.04.037
70. Kumstel J, Kirsch B (2013) Polishing titanium- and nickel-based alloys using Cw-laser radiation. Physics Procedia, Lasers in Manufacturing (LiM 2013) 41:362–371. https://doi.org/10.1016/j.phpro.2013.03.089
71. Temmler A, Willenborg E, Wissenbach K (2012) Laser polishing, in: Laser applications in microelectronic and optoelectronic manufacturing (LAMOM) XVII. Presented at the Laser Applications in Microelectronic and Optoelectronic Manufacturing (LAMOM) XVII, International Society for Optics and Photonics, p. 82430W. https://doi.org/10.1117/12.906001
72. Temmler A, Willenborg E, Wissenbach K (2012) Designing surfaces by laser remelting. https://doi.org/10.13140/2.1.1555.8409
73. Temmler A, Liu D, Preußner J, Oeser S, Luo J, Poprawe R, Schleifenbaum JH (2020) Influence of laser polishing on surface roughness and microstructural properties of the remelted surface boundary layer of tool steel H11. Mater Des 192:108689. https://doi.org/10.1016/j.matdes.2020.108689
74. Ramos JA, Murphy J, Wood K, Bourell DL, Beaman JJ (2001) Surface roughness enhancement of indirect-SLS metal parts by laser surface polishing. https://doi.org/10.26153/tsw/3233
75. Temple PA, Lowdermilk WH, Milam D (1982) Carbon dioxide laser polishing of fused silica surfaces for increased laser-damage resistance at 1064 nm. Appl Opt 21:3249–3255. https://doi.org/10.1364/AO.21.003249
76. Wang H-Y, Bourell DL, Beaman JJ (2003) Laser polishing of silica slotted rods. Mater Sci Technol 19:382–387. https://doi.org/10.1179/026708303225009760
77. Ramos JA, Bourell DL, Beaman JJ (2002) Surface over-melt during laser polishing of indirect-SLS metal parts. MRS Online Proceedings Library (OPL) 758. https://doi.org/10.1557/PROC-758-LL1.9
78. Shao TM, Hua M, Tam HY, Cheung EHM (2005) An approach to modelling of laser polishing of metals. Surf Coat Technol 197:77–84. https://doi.org/10.1016/j.surfcoat.2005.01.010
79. Gisario A, Bellisario D, Veniali F (2010) Thermal–morphological analysis of diode laser polishing on sintered bronze. Int J Mater Form 3:1067–1070. https://doi.org/10.1007/s12289-010-0955-1
80. Lamikiz A, Sanchez JA, De Lacalle LNL, Del Pozo D, Etayo JM, Lopez JM (2007) Laser polishing techniques for roughness improvement on metallic surfaces. Int J Nanomanuf 1:490–498. https://doi.org/10.1504/IJNM.2007.014568
81. Marinescu NI, Ghiculescu D, Jitianu G, Seritan G (2008) Improvement of technological parameters at surface finishing through laser beam machining. 6th International DAAAM Baltic Conference Industrial Engineering 24–26 April 2008, Tallinn, Estonia
82. Gisario A, Boschetto A, Veniali F (2011) Surface transformation of AISI 304 stainless steel by high power diode laser. Opt Lasers Eng 49:41–51. https://doi.org/10.1016/j.optlaseng.2010.09.001
83. Gisario A, Barletta M, Veniali F (2012) Surface reconstruction of porous substrates in sintered bronze by cw-high power diode laser. Opt Lasers Eng 50:1306–1315. https://doi.org/10.1016/j.optlaseng.2012.02.016
84. Lamikiz A, Sánchez JA, López de Lacalle LN, Arana JL (2007) Laser polishing of parts built up by selective laser sintering. Int J Mach Tools Manuf 47:2040–2050. https://doi.org/10.1016/j.ijmachtools.2007.01.013
85. Mohajerani S, Bordatchev EV, Tutunea-Fatan OR (2018) Recent developments in modeling of laser polishing of metallic materials. Lasers Manuf Mater Process 5:395–429. https://doi.org/10.1007/s40516-018-0071-5
86. Purushothaman S, Ravi Sankar M (2021) State of the art on atomistic modelling of laser polishing. Materials Today: Proceedings, International Conference on Materials, Processing & Characterization 44:689–695. https://doi.org/10.1016/j.matpr.2020.10.612
87. Xu J, Zou P, Wang W, Kang D (2021) Study on the mechanism of surface topography evolution in melting and transition regimes of laser polishing. Opt Laser Technol 139:106947. https://doi.org/10.1016/j.optlastec.2021.106947
88. Willenborg E (2011) Polishing with laser radiation. Poprawe R, ed. Tailored Light 2. Berlin: Springer, pp. 196–203
89. Temmler A, Liu DM, Drinck S, Luo JB, Poprawe R (2020) Experimental investigation on a new hybrid laser process for surface structuring by vapor pressure on Ti6Al4V. J Mater Process Technol 277:116450. https://doi.org/10.1016/j.jmatprotec.2019.116450
90. Temmler A, Willenborg E, Wissenbach K (2009) Structuring by remelting. Proceedings of the 5th Int. WLTConference on Lasers in Manufacturing, pp. 403–407
91. Laser Polishing of Metals - Brochure - Fraunhofer ILT [WWW Document] (n.d) Fraunhofer Institute for Laser Technology ILT. (Accessed 9.11.21) https://www.ilt.fraunhofer.de/en/media-center/brochures/brochure-laser-polishing-of-metals.html
92. Temmler A, Wei D, Schmickler T, Küpper M. E, Häfner CL (2020) Experimental investigation on surface structuring by laser remelting (Wave Shape) on Inconel 718 using varying laser beam diameters and scan speeds. Appl Surf Sci 147814. https://doi.org/10.1016/j.apsusc.2020.147814
93. Giorleo L, Ceretti E, Giardini C (2015) Ti surface laser polishing: effect of laser path and assist gas. Procedia CIRP, 9th CIRP Conference on Intelligent Computation in Manufacturing Engineering - CIRP ICME '14 33:446–451. https://doi.org/10.1016/j.procir.2015.06.102
94. Miller JD, Tutunea-Fatan OR, Bordatchev EV (2017) Experimental analysis of laser and scanner control parameters during laser polishing of H13 steel. Procedia Manufacturing, 45th SME North American Manufacturing Research Conference, NAMRC

45. LA, USA 10:720–729. https://doi.org/10.1016/j.promfg.2017.07.029
95. De Giorgi C, Furlan V, Demir AG, Tallarita E, Candiani G, Previtali B (2016) Laser micro-polishing of stainless steel for antibacterial surface applications. Procedia CIRP, The Second CIRP Conference on Biomanufacturing 49:88–93. https://doi.org/10.1016/j.procir.2015.07.055
96. Ukar E, Lamikiz A, Martínez S, Estalayo F, Tabernero I (2013) Laser polishing of GGG70L cast iron with 2D scan-head. Procedia Engineering, The Manufacturing Engineering Society International Conference, MESIC 2013(63):53–59. https://doi.org/10.1016/j.proeng.2013.08.199
97. Perry TL, Werschmoeller D, Li X, Pfefferkorn FE, Duffie NA (2009) Pulsed laser polishing of micro-milled Ti6Al4V samples. J Manuf Process 11:74–81. https://doi.org/10.1016/j.jmapro.2009.10.001
98. Obeidi MA, McCarthy E, O'Connell B, Ul Ahad I, Brabazon D (2019) Laser polishing of additive manufactured 316L stainless steel synthesized by selective laser melting. Materials 12:991. https://doi.org/10.3390/ma12060991
99. Blakey-Milner B, Gradl P, Snedden G, Brooks M, Pitot J, Lopez E, Leary M, Berto F, du Plessis A (2021) Metal additive manufacturing in aerospace: a review. Mater Des 209:110008. https://doi.org/10.1016/j.matdes.2021.110008
100. Gisario A, Kazarian M, Martina F, Mehrpouya M (2019) Metal additive manufacturing in the commercial aviation industry: a review. J Manuf Syst 53:124–149
101. Liu R, Wang Z, Sparks T, Liou F, Newkirk J (2017) 13 - Aerospace applications of laser additive manufacturing. In: Brandt M (Ed.) Laser additive manufacturing, woodhead publishing series in electronic and optical materials. Woodhead Publishing, pp. 351–371. https://doi.org/10.1016/B978-0-08-100433-3.00013-0
102. Dadbakhsh S, Speirs M, Humbeeck JV, Kruth J-P (2016) Laser additive manufacturing of bulk and porous shape-memory NiTi alloys: from processes to potential biomedical applications. MRS Bull 41:765–774. https://doi.org/10.1557/mrs.2016.209
103. Munsch M (2017) Laser additive manufacturing of customized prosthetics and implants for biomedical applications. In: Brandt M (Ed.) Laser additive manufacturing, Woodhead Publishing Series in Electronic and Optical Materials. Woodhead Publishing, pp. 399–420. https://doi.org/10.1016/B978-0-08-100433-3.00015-4
104. Basha SM, Bhuyan M, Basha MM, Venkaiah N, Sankar MR (2020) Laser polishing of 3D printed metallic components: a review on surface integrity. Materials Today: Proceedings, 10th International Conference of Materials Processing and Characterization 26:2047–2054. https://doi.org/10.1016/j.matpr.2020.02.443
105. Li Y-H, Wang B, Ma C-P, Fang Z-H, Chen L-F, Guan Y-C, Yang S-F (2019) Material characterization, thermal analysis, and mechanical performance of a laser-polished Ti alloy prepared by selective laser melting. Metals 9:112. https://doi.org/10.3390/met9020112
106. Tian Y, Gora WS, Cabo AP, Parimi LL, Hand DP, Tammas-Williams S, Prangnell PB (2018) Material interactions in laser polishing powder bed additive manufactured Ti6Al4V components. Addit Manuf 20:11–22. https://doi.org/10.1016/j.addma.2017.12.010
107. Xu Z, Ouyang W, Liu Y, Jiao J, Liu Y, Zhang W (2020) Effects of laser polishing on surface morphology and mechanical properties of additive manufactured TiAl components, in: 24th National Laser Conference & Fifteenth National Conference on Laser Technology and Optoelectronics. Presented at the 24th National Laser Conference & Fifteenth National Conference on Laser Technology and Optoelectronics, International Society for Optics and Photonics, p. 117172Y. https://doi.org/10.1117/12.2587455
108. Zhihao F, Libin L, Longfei C, Yingchun G (2018) Laser polishing of additive manufactured superalloy. Procedia CIRP, 4th CIRP Conference on Surface Integrity (CSI 2018) 71:150–154. https://doi.org/10.1016/j.procir.2018.05.088
109. Chandler H (1996) Heat treater's guide: practices and procedures for nonferrous alloys. ASM International
110. Chen L, Richter B, Zhang X, Ren X, Pfefferkorn FE (2020) Modification of surface characteristics and electrochemical corrosion behavior of laser powder bed fused stainless-steel 316L after laser polishing. Addit Manuf 32:101013. https://doi.org/10.1016/j.addma.2019.101013
111. dos Santos Solheid J, Seifert HJ, Pfleging W (2018) Laser surface modification and polishing of additive manufactured metallic parts. Procedia CIRP, 10th CIRP Conference on Photonic Technologies [LANE 2018] 74:280–284. https://doi.org/10.1016/j.procir.2018.08.111
112. Schanz J, Hofele M, Hitzler L, Merkel M, Riegel H (2016) Laser polishing of additive manufactured AlSi10Mg parts with an oscillating laser beam, in: Öchsner A, Altenbach H (Eds.) Machining, joining and modifications of advanced materials, advanced structured materials. Springer, Singapore, pp. 159–169. https://doi.org/10.1007/978-981-10-1082-8_16
113. Yung KC, Xiao TY, Choy HS, Wang WJ, Cai ZX (2018) Laser polishing of additive manufactured CoCr alloy components with complex surface geometry. J Mater Process Technol 262:53–64. https://doi.org/10.1016/j.jmatprotec.2018.06.019
114. Wang WJ, Yung KC, Choy HS, Xiao TY, Cai ZX (2018) Effects of laser polishing on surface microstructure and corrosion resistance of additive manufactured CoCr alloys. Appl Surf Sci 443:167–175. https://doi.org/10.1016/j.apsusc.2018.02.246
115. Dadbakhsh S, Hao L, Kong CY (2010) Surface finish improvement of LMD samples using laser polishing. Virtual and Physical Prototyping 5:215–221. https://doi.org/10.1080/17452759.2010.528180
116. Rosa B, Mognol P, Hascoët J (2015) Laser polishing of additive laser manufacturing surfaces. J Laser Appl 27:S29102. https://doi.org/10.2351/1.4906385
117. Bhaduri D, Penchev P, Batal A, Dimov S, Soo SL, Sten S, Harrysson U, Zhang Z, Dong H (2017) Laser polishing of 3D printed mesoscale components. Appl Surf Sci 405:29–46. https://doi.org/10.1016/j.apsusc.2017.01.211
118. Marimuthu S, Triantaphyllou A, Antar M, Wimpenny D, Morton H, Beard M (2015) Laser polishing of selective laser melted components. Int J Mach Tools Manuf 95:97–104. https://doi.org/10.1016/j.ijmachtools.2015.05.002
119. Witkin DB, Patel DN, Helvajian H, Steffeney L, Diaz A (2019) Surface treatment of powder-bed fusion additive manufactured metals for improved fatigue life. J of Materi Eng and Perform 28:681–692. https://doi.org/10.1007/s11665-018-3732-9
120. Witkin D, Helvajian H, Steffeney L, Hansen W (2016) Laser post-processing of Inconel 625 made by selective laser melting, in: Laser 3D manufacturing III. Presented at the Laser 3D Manufacturing III, International Society for Optics and Photonics, p. 97380W. https://doi.org/10.1117/12.2213745
121. Kahlin M, Ansell H, Basu D, Kerwin A, Newton L, Smith B, Moverare JJ (2020) Improved fatigue strength of additively manufactured Ti6Al4V by surface post processing. Int J Fatigue 134:105497. https://doi.org/10.1016/j.ijfatigue.2020.105497
122. Liang C, Hu Y, Liu N, Zou X, Wang H, Zhang X, Fu Y, Hu J (2020) Laser polishing of Ti6Al4V fabricated by selective laser melting. Metals 10:191. https://doi.org/10.3390/met10020191
123. Lee S, Ahmadi Z, Pegues JW, Mahjouri-Samani M, Shamsaei N (2021) Laser polishing for improving fatigue performance of additive manufactured Ti-6Al-4V parts. Opt Laser Technol 134:106639. https://doi.org/10.1016/j.optlastec.2020.106639
124. Alfieri V, Argenio P, Caiazzo F, Sergi V (2017) Reduction of surface roughness by means of laser processing over additive

manufacturing metal parts. Materials 10:30. https://doi.org/10.3390/ma10010030
125. Shah LH, Khodabakhshi F, Gerlich A (2019) Effect of beam wobbling on laser welding of aluminum and magnesium alloy with nickel interlayer. J Manuf Process 37:212–219. https://doi.org/10.1016/j.jmapro.2018.11.028
126. Kuryntsev SV, Gilmutdinov AKh (2015) The effect of laser beam wobbling mode in welding process for structural steels. Int J Adv Manuf Technol 81:1683–1691. https://doi.org/10.1007/s00170-015-7312-y
127. Yasa E, Kruth J-P (2011) Application of laser re-melting on selective laser melting parts. Advances in Production Engineering and Management 6:259–270
128. Alrbaey K, Wimpenny D, Tosi R, Manning W, Moroz A (2014) On optimization of surface roughness of selective laser melted stainless steel parts: a statistical study. J of Materi Eng and Perform 23:2139–2148. https://doi.org/10.1007/s11665-014-0993-9
129. Ukar E, Lamikiz A, Martínez S, Tabernero I, de Lacalle LNL (2012) Roughness prediction on laser polished surfaces. J Mater Process Technol 212:1305–1313. https://doi.org/10.1016/j.jmatprotec.2012.01.007
130. Caggiano A, Teti R, Alfieri V, Caiazzo F (2021) Automated laser polishing for surface finish enhancement of additive manufactured components for the automotive industry. Prod Eng Res Devel 15:109–117. https://doi.org/10.1007/s11740-020-01007-1
131. Bordatchev E, Hafiz A, Tutunea-Fatan OR (2014) Performance of laser polishing in finishing of metallic surfaces. The International Journal of Advanced Manufacturing Technology 73:35–52. https://doi.org/10.1007/s00170-014-5761-3
132. Ahmed W, Elhissi A, Jackson MJ, Ahmed E (2012) Precision machining of medical devices. In: Davim JP (Ed.) The design and manufacture of medical devices. Woodhead Publishing Reviews: Mechanical Engineering Series. Woodhead Publishing, pp. 59–113. https://doi.org/10.1533/9781908818188.59
133. Ma CP, Guan YC, Zhou W (2017) Laser polishing of additive manufactured Ti alloys. Opt Lasers Eng 93:171–177. https://doi.org/10.1016/j.optlaseng.2017.02.005
134. Flemmer J, Ross I, Willenborg E, Fröba H (2015) Machine tool and CAM-NC data chain for laser polishing complex shaped parts. Adv Eng Mater 17:260–267. https://doi.org/10.1002/adem.201400476
135. Kreinest L, Sängerlaub S, Willemborg E (2020) Laser polishing of metallic 3D parts – process, CAM-NC and machine. Presented at the Virtual Conference: LaP 2020, 4TH Conference on Laser Polishing
136. Mehta B (2020) Enhanced performance of magnetic floating devices enabled through metal additive manufacturing
137. Mehta B, Hryha E, Nyborg L, Tholence F, Johansson E (2021) Effect of surface sandblasting and turning on compressive strength of thin 316L stainless steel shells produced by laser powder bed fusion. Metals 11:1070. https://doi.org/10.3390/met11071070
138. Yasa E, Deckers J, Kruth J (2011) The investigation of the influence of laser re-melting on density, surface quality and microstructure of selective laser melting parts. Rapid Prototyping Journal 17:312–327. https://doi.org/10.1108/13552541111156450